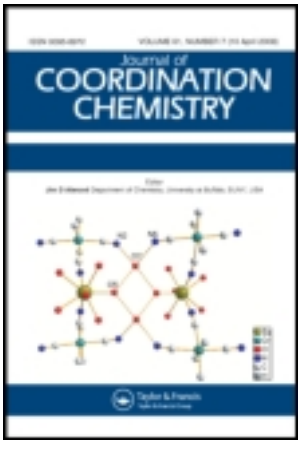

Journal of Coordination Chemistry
Publication details, including instructions for authors and subscription information:
http://www.tandfonline.com/loi/gcoo20

Protonation and coordination ability of small peptides - theoretical and experimental approaches for elucidation

Marc Lamshöft [a] & Bojidarka Ivanova [a]

[a] Institute of Environmental Research of the Faculty of Chemistry, Dortmund University of Technology , Otto-Hahn-Str. 6, D-44227 Dortmund, Germany

Published online: 13 Jul 2011.

To cite this article: Marc Lamshöft & Bojidarka Ivanova (2011) Protonation and coordination ability of small peptides - theoretical and experimental approaches for elucidation, Journal of Coordination Chemistry, 64:14, 2419-2442, DOI: 10.1080/00958972.2011.598926

To link to this article: http://dx.doi.org/10.1080/00958972.2011.598926

Journal of Coordination Chemistry
Vol. 64, No. 14, 20 July 2011, 2419–2442

REVIEW

Protonation and coordination ability of small peptides – theoretical and experimental approaches for elucidation

MARC LAMSHÖFT and BOJIDARKA IVANOVA*

Institute of Environmental Research of the Faculty of Chemistry, Dortmund University of Technology, Otto-Hahn-Str. 6, D-44227 Dortmund, Germany

(*Received 5 October 2010; in final form 4 April 2011*)

This review deals with modern theoretical and experimental approaches as well as structural elucidation of small peptides (SP), their protonated forms and metal complexes. Free peptide bond rotation in amino acids (AA) and peptides yielded various conformers, which may possess differing biological activities. Inter- and/or intramolecular stacking observed in aromatic SP is another phenomenon typical for both peptide salts and complexes. These phenomenological effects can be successfully studied, both theoretically and experimentally, using a combination of the theoretical approximations and physical methods, such as electronic absorption spectroscopy, vibrational spectroscopy (including IR and Raman), nuclear magnetic resonance, mass spectrometry, as well as single-crystal X-ray diffraction. The physical and chemical properties of these systems can be precisely calculated by *ab initio* and DFT methods, varying basis sets and the results obtained allow elucidation of their conformations as a function of the reaction conditions (pH, type of the solvent, temperature, metal to ligand molar ratio). Although the 3-D structures of many peptides have been determined over the past decades, peptide crystallization is still a major obstacle to crystallographic work and the presence of chiral center/s adds further difficulties. For this reason, a specific part of the review is focused on the study of the absolute structure of the peptides, their salts and metal complexes, discussing the conformational preferences of the peptides during these processes. The available crystallographic data for metal complexes are successfully used for the correlation between the structures and the spectroscopic properties.

Keywords: Metal complexes; Small peptides; Structural and spectroscopic study; NLO materials

1. Introduction

Free peptide bond rotation yields various conformers, which as a result of protonation or coordination processes, possess differing biological activities. Intermolecular aromatic stacking in aromatic small peptides (SP) is another interesting phenomenon with an important role in biological systems [1–4]. It provides a reasonable explanation for the function and selectivity of variable ion channels [5–16]. On the other hand, one of the fast developing areas on design and synthesis of new organic non-linear optical (NLO) materials is focused on tuning of the spectroscopic properties and crystal

*Corresponding author. Email: B.Ivanova@web.de; B.Ivanova@infu.tu-dortmund.de; B.Ivanova@infu.uni-dortmund.de

ISSN 0095-8972 print/ISSN 1029-0389 online
DOI: 10.1080/00958972.2011.598926

packing in derivatives of amino acids(AA) and SP [17–39], whose molecular conformation is changed dramatically during coordination with metal ions. A great number of SP/metal complexes have been reported. The main focus of these investigations, however, has been of outstanding biological significance [40–86]. We will try to make a parallel between the fundamental aspects of the molecular conformation of SP and the large number of the studies on their coordination and protonation ability.

The review highlights SP with aliphatic and aromatic residues, with the purpose of focusing the reader's attention on specific phenomena typical only of these systems as well as common phenomena related to their coordination and/or protonation ability. Data include a series of more than 50 peptides, containing *Gly*, *Ala*, *Met*, *Trp*, *Tyr*, *Phe*, *Thr*, and *Ser* residues. It is clear from all available studies that SP are very efficient and versatile ligands for complexation with M^{II} ions, whose conformations can be studied as a function of pH, where the presence of only one amide fragment in the molecules allows precise elucidation of the conformational changes. The effect on identical structural fragments is typical for peptides with large numbers of AA residues, and we will focus mainly on the di- and tripeptide systems. We will perform a parallel description within their molecular geometries and properties, and those of the peptide analogs containing up to six AA residues.

2. Protonation ability of SP

2.1. *Experimental characterization*

2.1.1. Characterization by vibrational (IR and Raman) spectroscopy. The main vibrational characteristics, for both IR and Raman, are for the $-NH_3^+$, $-COO^-$, and amide (HNC(=O)) groups in the zwitterionic peptides, observed within the same spectroscopic regions (table 1) [18–39, 45–107]. Study of the protonated forms of SP in parallel with coordination properties allows a better understanding of the complexation processes, since protonation leads to the formation of COOH-group in the preliminary zwitterionic peptide such as for monodentate coordination through the O-center of $-COO^-$ group. The manner, especially when these systems interact with the ions such as Cu^{II}, Co^{II}, or Ni^{II}, strongly depends on the pH of the solution, thus giving the possibility of parallel formation/isolation of the salts of the peptides in solid state. The vibrational spectra of the salts, independent of the type of counterion [18–39], showed strong overlapping IR spectral curves which required further application of mathematical procedures [108–111]. In spite of the equivalent side chains included in the structures of SP or their protonated forms, the IR spectral characteristics differ because of different types of intermolecular interactions in the solid state (table 1). The disappearance of the bands for asymmetric and symmetric stretching vibration of the $-COO^-$ group ($\nu^{as}_{COO^-}$, $\nu^{s}_{COO^-}$) [112–115] and the observation of a new peak at 1750 cm^{-1}, associated with the $\nu_{C=O}$ stretching of –COOH group, is common for all the salts. The bands at 3288 cm^{-1} (ν_{NH}) and amide I at 1656 cm^{-1} (figure 1) in the *H–(Gly)$_2$–OH* are typical for the flat *trans*-amide fragment. This result is in accord with known crystallographic data for *H–(Gly)$_2$–OH*, indicating a C(=O)–NH angle of 178.7° [113] (figure 1). The protonation of the peptide led to a shift of corresponding amide vibrations

Table 1. Characteristic IR-bands of neutral glycine homopeptides in the solid state.

	ν (cm^{-1})					
Assignment	*H–(Gly)$_2$–OH*	*H–(Gly)$_3$–OH*	*H–(Gly)$_4$–OH*	*H–(Gly)$_5$–OH*	*H–(Gly)$_6$–OH*	
ν_{NH}	3288	3316, 3298	3335, 3294, 3283	3302, 3298, 3284, 3269	3332, 3327, 3310, 3300, 3275	
ν^{as}_{NH3+}, ν^{s}_{NH3+}	3200–2400	3200–2400	3200–2400	3100–2500	3200–2400	
δ^{as}_{NH3+}	1679, 1673	1681, 1621	1675, 1688	1698, 1688	1690, 1689	
$\nu_{C=O}$ (amide I)	1656	1657, 1646	1662, 1646, 1638	1684, 1674, 1659, 1632	1686, 1676, 1660, 1635, 1627	
$\nu^{as}_{COO^-}$	1533	1534	1563	1563	1560	
δ_{NH} (amide II)	1554	1556, 1519	1579, 1554, 1535	1578, 1568, 1561, 1541	1548, 1537, 1524, 1513, 1502	
δ^{s}_{NH3+}	1500	1506	1469	1529	1527	
$\nu^{s}_{COO^-}$	1409	1400	1415	1413	1405	
ν_{CN} (amide III)	1253	1228	1245 with submaxima	1252	1288	
γ_{NH} (amide V)	713	696, 690	719, 699, 683	727, 722, 713, 700	727, 720, 692, 694, 672	
$\delta_{C=O}$ (amide IV)	663	644, 640	667, 651, 647	681, 666, 614, 610	684, 681, 677, 673, 666	
Assignment	*H–Gly–Ala–OH*	*H–Gly–(Ala)$_2$–OH*	*H–Ala–Phe–OH*	*H–Ala–Phe–OH · HCl*	*H–Phe–Ala–OH · 2H$_2$O*	*H–Phe–Ala–OH·HCl*
ν_{NH3+}	3300–2300			3200–2700		
ν^{as}_{NH3+}	3048	3085				
ν_{NH}	3216	3284, 3235	3250	3261	3280	3203
ν_{OH}	–	–	–	–	3360 (H_2O)	3401 (COOH)
$\nu_{C=O}$ (COOH)	–	–	–	1725	–	1737
$\nu_{C=O}$ (amide I)	1683	1681, 1648	1675	1658	1677	1670
δ^{as}_{NH3+}, δ'_{NH3+}as	1643, 1640	1671, 1675	1693, 1681	1691, 1685	1664, 1660	1654, 1650
δ_{NH2}	–	–	–	–	–	–
δ^{s}_{NH3+}	1585	1610	1625	1623	1546	1511
$\nu^{as}_{COO^-}$	1562	1596	1521	–	1610	–
δ_{NH} (amide II)	1533	1560, 1556	1560	1545	1525	1571
$\nu^{s}_{COO^-}$	1409	1425	1388	–	1401	–

(*Continued*)

Table 1. Continued.

Assignment		Assignment		Assignment		Assignment	
H–Trp–Met–OH				*H–Met–Trp–OH*			
ν_{NH}	3326	$\nu^{s}_{COO^-}$	1396	ν_{NH}	3446	$\nu^{s}_{COO^-}$	1406
$\nu_{NH(In)}$	3409	$\nu_{C–N}/\delta_{NH\ (amide\ III)}$	1257	$\nu_{NH(In)}$	3424	$\nu_{C–N}/\delta_{NH\ (amide\ III)}$	1260
$\nu_{OH(H2O)}$	–	$\nu_{N–C}$	1000	$\nu_{OH(H2O)}$	–	$\nu_{N–C}$	1008
ν^{as}_{NH3+}, ν^{s}_{NH3+}	3190	Indole o.p.	738, 424	ν^{as}_{NH3+}, ν^{s}_{NH3+}	3208	Indole o.p.	742, 420
δ_{NH3+}	1675	$\nu_{S–C(H3)}$	721	δ_{NH3+}	1685	$\nu_{S-C(H3)}$	723
$\nu_{C=O\ (amide\ I)}$	1662	$\delta_{COO–}$	684	$\nu_{C=O\ (amide\ I)}$	1675	$\delta_{COO–}$	661
δ^{as}_{NH3+}	1623	$\rho_{COO–}$	505	δ^{as}_{NH3+}	1643	$\rho_{COO–}$	484
Indole i.p.	1612, 1469, 1265	$\gamma_{NH\ (amide\ V)}$	651	Indole i.p.	1615, 1465, 1265	$\gamma_{NH\ (amide\ V)}$	665
$\nu^{as}_{COO^-}$	1581	$\delta_{C=O\ (amide\ IV)}$	580	$\nu^{as}_{COO^-}$	1615	$\delta_{C=O\ (amide\ IV)}$	640
$\delta_{NH\ (amide\ II)}$	1521	$\gamma_{C=O\ (amide\ VI)}$	526	$\delta_{NH\ (amide\ II)}$	1508	$\gamma_{C=O\ (amide\ VI)}$	560

Assignment		Assignment									
H–Gly–Trp–OH · 2H$_2$O					*Phe*	*Tyr*	*Trp*		*Phe*	*Tyr*	*Trp*
ν_{NH}	3430	$\nu^{s}_{COO^-}$	1395	ν_{NHInd}	–	–	1495 ± 03	$\nu_{Ph/(r)}$	1485 ± 03	3402 ± 03	1525 ± 05
$\nu_{NH(In)}$	3419	$\nu_{C–N}/\delta_{NH\ (amide\ III)}$	1255	$\nu_{CH/(r)}$	3085 ± 05	3090 ± 05	1500 ± 05	$\nu_{Ph/(r)}$	1500 ± 05	3050 ± 05	1480 ± 05
$\nu_{OH(H2O)}$	3280	$\nu_{N–C}$	1010	$\nu_{CH/(r)}$	3070 ± 05	3070 ± 05	830 ± 15	$\gamma_{CH/(r)}$	770 ± 05	3020 ± 05	744 ± 05
ν^{as}_{NH3+}, ν^{s}_{NH3+}	3210	Indole o.p.	750, 424	$\nu_{CH/(r)}$	3060 ± 05	3050 ± 05	640 ± 15	$\delta_{ph/(r)}$	750 ± 05	2995 ± 05	695 ± 05
δ_{NH3+}	1689	$\nu_{S–C(H3)}$	718	$\nu_{Ph/(r)}$	1605 ± 03	1600 ± 03	700 ± 10	$\gamma_{Ph/(r)}$	695 ± 02	1624 ± 05	640 ± 05
$\nu_{C=O\ (amide\ I)}$	1673	$\delta_{COO–}$	696	$\nu_{Ph/(r)}$	1585 ± 05	1580 ± 05	–	δ_{NHInd}	–	1575 ± 05	575 ± 30, 555 ± 15
δ^{as}_{NH3+}	1617	$\rho_{COO–}$	468	–	–	–	–	–	–	–	–
Indole i.p.	1610, 1465, 1265	$\gamma_{NH(amide\ V)}$	474	–	–	–	–	–	–	–	–
$\nu^{as}_{COO^-}$	1563	$\delta_{C=O(amide\ IV)}$	576	–	–	–	–	–	–	–	–
$\delta_{NH\ (amide\ II)}$	1540	$\gamma_{C=O(amide\ VI)}$	553	–	–	–	–	–	–	–	–

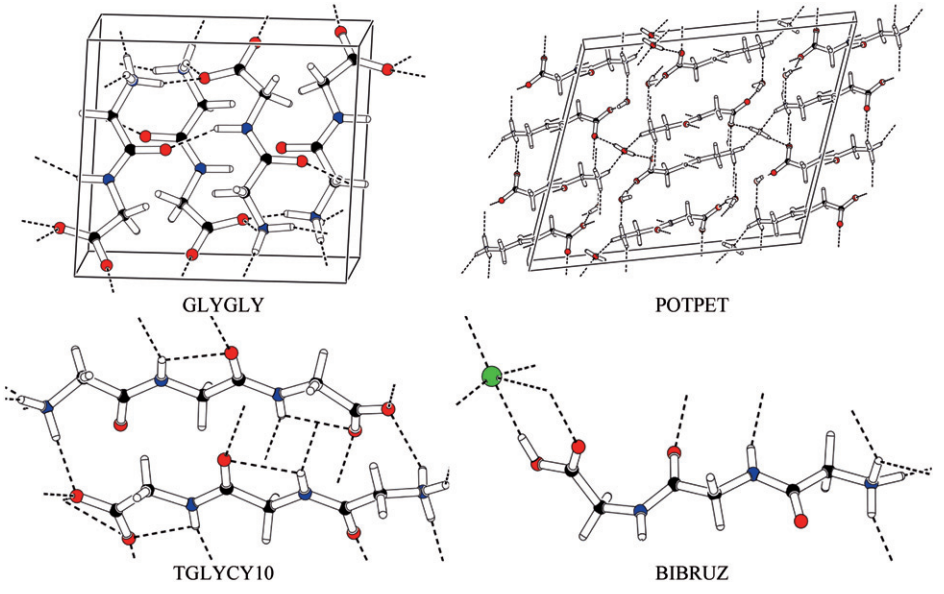

Figure 1. Crystallographic data for *H–(Gly)$_2$–OH* (GLYGLY), *H–(Gly)$_2$–OH* dihydrate (POTPET) [114], *H–(Gly)$_3$–OH* (TGLYCY10), and *H–(Gly)$_3$–OH·HCl* (BIBRUZ). The crystal structures are given by their CCDC codes (http://www.ccdc.cam.ac.uk/).

on account of the effect of the different types of intermolecular hydrogen-bonding networks in the crystals (figure 1). Similarly, in the ionized form $\nu_{C=O}$ and ν_{NH} in *H–(Gly)$_2$–OH.HCl* are observed at 1670 and 3278 cm^{-1}, indicating a flat *trans*–C(=O)–NH group with torsion angle of 170.5° [115] with a shift of about 14 cm^{-1} of $\nu_{C=O}$. The new band at 1749 cm^{-1} corresponds to the $\nu_{C=O}$ of the –COOH fragment.

The data for the higher *Gly*-analogs revealed that the values for δ_{NH} are typical of *trans*-amide fragments where the frequency of the IR band corresponding to δ_{NH} is observed within the range of 1560–1530 cm^{-1} (table 1) [116–135]. However, the strong overlapping of the spectroscopic patterns requires the application of other physical methods, such as NMR and MS. In parallel to the experimental study, the theoretical approaches for predicting the molecular geometry and physical properties of these complicated systems were also successfully employed and thus, their complete characterizations were made possible [136–169]. The *Ala*-residue has a weak effect (table 2) at 1640 cm^{-1} (*H–Gly–Ala–OH*) and at 1670 cm^{-1} (*H–Gly–(Ala)$_2$–OH*) for bending and stretching vibrations of the NH_3^+-group: at 3200 (ν_{NH}), 1690–1640 ($\nu_{C=O}$), and 1560 cm^{-1} (δ_{NH}). The $\nu^{as}_{COO^-}$ and $\nu^{s}_{COO^-}$ are observed at 1590–1560 and 1420 cm^{-1} (table 1).

Vibrational properties of *H–Thr–Ser–OH* are: a broad band at 3200–2600 cm^{-1} (vibrations of $-NH_3^+$-group, table 2), δ^{as}_{NH3+}, δ'_{NH3+}as, and δ^{s}_{NH3+} bands (1614, 1515 cm^{-1}), ν_{OH} and ν_{NH} modes at 3390, 3335, and 3288 cm^{-1}, respectively. The *Ser* ν_{OH} is observed at 3357 cm^{-1} in the pure AA. The band at 1644 cm^{-1} can be assigned to amide I and the 1558 cm^{-1} to amide II. $\nu^{as}_{COO^-}$ and $\nu^{s}_{COO^-}$ are associated with maxima at 1560 and 1400 cm^{-1}, respectively, which disappear in the protonated dipeptide. In *Ser* these peaks are at 1622 and 1416 cm^{-1}, respectively. Protonation of *H–Thr–Ser–OH.HSq* led to disappearance of $\nu^{as}_{COO^-}$ and $\nu^{s}_{COO^-}$. New peaks at 1700 and 1745 cm^{-1}

Table 2. Characteristic normal vibrations for the common functional groups in the zwitterionic peptides.

$-COO^-$		–COOH		$-NH_3^+$		$-NH_2$		Amide (–NHC(=O))		
Vibration	ν (cm^{-1})	Vibration	ν (cm^{-1})	Vibration	ν (cm^{-1})	Vibration	ν (cm^{-1})	Vibration	ν (cm^{-1})	
$\nu^{as}_{COO^-}$	1580 ± 35	$\nu_{OH\ (bonded)}$	3055 ± 50	ν^{as}_{NH3+}	3155 ± 50	ν^{as}_{NH2}	3365 ± 30	$\nu_{NH\ (A)}$	3400 ± 50	
$\nu^{s}_{COO^-}$	1410 ± 30	$\nu_{C=O}$	1735 ± 50	$\nu^{as'}_{NH3+}$	3055 ± 70	ν^{s}_{NH2}	3280 ± 30	$\nu_{C=O}$	1680 ± 50	Amide I
δ_{COO-}	740 ± 100	ν_{C-O}	1240 ± 80	ν^{s}_{NH3+}	2950 ± 50	δ_{NH2}	1610 ± 15	δ_{NH}	1550 ± 50	Amide II
ω_{COO-}	650 ± 20	$\delta_{C=O}$	700 ± 80	δ^{as}_{NH3+}	1610 ± 25	τ/ρ_{NH2}	1220 ± 70	ν_{C-N}	1270 ± 50	Amide III
ρ_{COO-}	530 ± 60	$\gamma_{C=O}$	580 ± 100	$\delta^{as'}_{NH3+}$	1585 ± 25	ω_{NH2}	850 ± 50	$\delta_{C=O}$	690 ± 70	Amide IV
–	–	–	–	δ^{s}_{NH3+}	1500 ± 30	–	–	$\omega_{NH2/CX}$	735 ± 60	Amide V
–	–	–	–	ρ_{NH3+}	1155 ± 50	–	–	$\gamma_{C=O}$	600 ± 60	Amide IV
–	–	–	–	–	–	–	–	$\tau_{NH2/CX}$	350 ± 50	Amide VII

of the $\nu_{C=O}$ vibrations as well as a low-frequency shifted amide I peak of 10 cm^{-1} as a result of a C=O···X intermolecular interaction were observed. Other characteristic maxima are at 2933 (ν_{NH}), 1637 (amide I), 1575 (δ^{as}_{NH3+}), and 1566 cm^{-1} (amide II). The series of IR bands, characteristic for *HSq*$^-$ ion are at 1820, 1600, and 1500 cm^{-1} assigned to the combination of ν_{C-O}, ν_{C-C}, and $\nu_{C=C}$ modes, respectively.

The presence of aromatic AA residues such as *Phe*, *Tyr*, or the indole skeleton in *Trp* additionally complicates the vibrational patterns of the corresponding peptides. These fragments are characterized by a series of bands of stretching and bending i.p. and o.p. vibrations, observed within the regions summarized in table 1.

Spectra of *H–Phe–Tyr–OH* and *H–Tyr–Phe–OH* showed peaks at 3290–3180 cm^{-1} ($\nu_{OH(solvent)}$, ν_{NH}, $\nu_{OH(Tyr)}$), at 3080–3050 cm^{-1} (δ^{as}_{NH3+}) [170–173], and at 1700 cm^{-1} ($\nu_{C=O(COOH)}$) in the protonated forms. The bands within the 1800–1500 cm^{-1} region are assigned as follows: *H–Tyr–Phe–OH*: 1675 cm^{-1} ($\nu_{C=O}$), 1613 cm^{-1} (**8a**, i.p.), 1597 cm^{-1} (**8b**, i.p.), 1571 cm^{-1} (**19a**$_{(Phe)}$, i.p.), 1562 cm^{-1} ($\nu^{as}_{COO^-}$), 1550 cm^{-1} (δ_{NH}) and 1517 cm^{-1} (**19a**$_{(Tyr)}$); *Tyr–Phe* salt: 1654 cm^{-1} (amide I), 1643 cm^{-1} (δ^{as}_{NH3+}), 1612 cm^{-1} (**8a**), 1590 cm^{-1} (**8b**$_{(Phe)}$), 1580 cm^{-1} (**8b**$_{(Tyr)}$), 1571 cm^{-1} (**19 a**$_{(Phe)}$), 1557 cm^{-1} (amide II), 1517 cm^{-1} (**19a**$_{(Tyr)}$); *H–Phe–Tyr–OH*: 1681 cm^{-1} (δ^{as}_{NH3+}), 1670 cm^{-1} (amide I), 1630 cm^{-1} (**8a**$_{(Phe)}$), 1614 cm^{-1} (**8a**$_{(Tyr)}$), 1594 cm^{-1} (**8b**$_{(Phe)}$), 1585 cm^{-1} (**8b**$_{(Tyr)}$), 1564 cm^{-1} (**19a**$_{(Phe)}$), 1554 cm^{-1} (amide II), 1525 cm^{-1} ($\nu^{as}_{COO^-}$), 1511 cm^{-1} (**19a**$_{(Tyr)}$); *Phe-Tyr salt*: 1656 cm^{-1} (δ^{as}_{NH3+}), 1650 cm^{-1} (amide I), 1612 cm^{-1} (**8a**), 1593 cm^{-1} (**8b**$_{(Phe)}$), 1587 cm^{-1} (**8b**$_{(Tyr)}$), 160 cm^{-1} (amide II), 1514 cm^{-1} (**19a**$_{(Tyr)}$), 1498 cm^{-1} (**19a**$_{(Phe)}$).

Intermolecular interactions in the *H–Tyr–Phe–OH* and its protonated form were determined from crystallographic data: $NH_{(amide)}$···O (2.853 Å), $OH_{(tyr)}$···O (2.614 Å), $NH_{(amino)}$···O (2.602 Å). The Cl^- and the protonated COOH group in the salt yielded (CO)OH···O (2.591 Å), $NH_{(amide)}$···Cl (3.156 Å), $C{=}O_{(amide)}$···H (2.591 Å), $OH_{(tyr)}$···O (3.151 Å), $NH_{(amino)}$···O (3.062–2.876 Å) and $NH_{(amino)}$···Cl (3.054 Å) bonds. The shorter length of the hydrogen bond with participation of $NH_{(amide)}$ in the non-protonated dipeptide explained the low-frequency shift of ν_{NH} to 3265 cm^{-1} (3275 cm^{-1} in the salt). In contrast, the $C{=}O_{(amide)}$ intermolecular interactions in the latter compound resulted in a low-frequency shift of amide I mode ($\nu_{C=O}$) to 1656 cm^{-1} (1675 cm^{-1} in *H–Tyr–Phe–OH*).

Protonation of the COO^- group in *H–Phe–Tyr–OH* resulted in significant changes in the IR spectrum of the salt, since the amide ν_{NH} and $\nu_{C=O}$ are low-frequency shifted to 3200 and 1650 cm^{-1}, indicating stronger intermolecular hydrogen bonds. The band at 1731 cm^{-1} belongs to $\nu_{C=O(COOH)}$, while the maximum at 3220 cm^{-1} is for ν_{NH}.

Characteristic vibrations of *H–Trp–Met–OH*, *H–Met–Trp–OH*, and *H–Gly–Trp–OH·2H$_2$O* (table 1) showed ν_{NH} within the 3326–3446 cm^{-1} range. The $\nu_{NH(In)}$, usually observed as a strong band, is located between 3409 and 3424 cm^{-1}. In all cases ν^{as}_{NH3+} and ν^{s}_{NH3+} vibrations were observed as broad bands within the 3200–2000 cm^{-1} range with highest frequency sub-maxima at about 3200 cm^{-1}. The 1800–1450 cm^{-1} region is characterized by overlapping absorptions of bending NH_3^+, $\nu_{C=O}$, $\nu^{as}_{COO^-}$, δ_{NH} and *In* i.p. vibrations. The 800–400 cm^{-1} region was analyzed and assigned to the o.p. vibrations of *In* ring, bending vibrations of COO^--group and amide IV–VI vibrations. The *In* o.p. mode at 740 cm^{-1} showed the greatest intensity within this region.

The IR-spectrum of *H–Trp–Met–OH* contained the ν_{NHIn} vibration as a low-intensity band (table 1), which could be explained by participation of the NH_{In} group in intermolecular interactions in the solid state. The band at 1662 cm^{-1} ($\nu_{C=O}$) indicates a

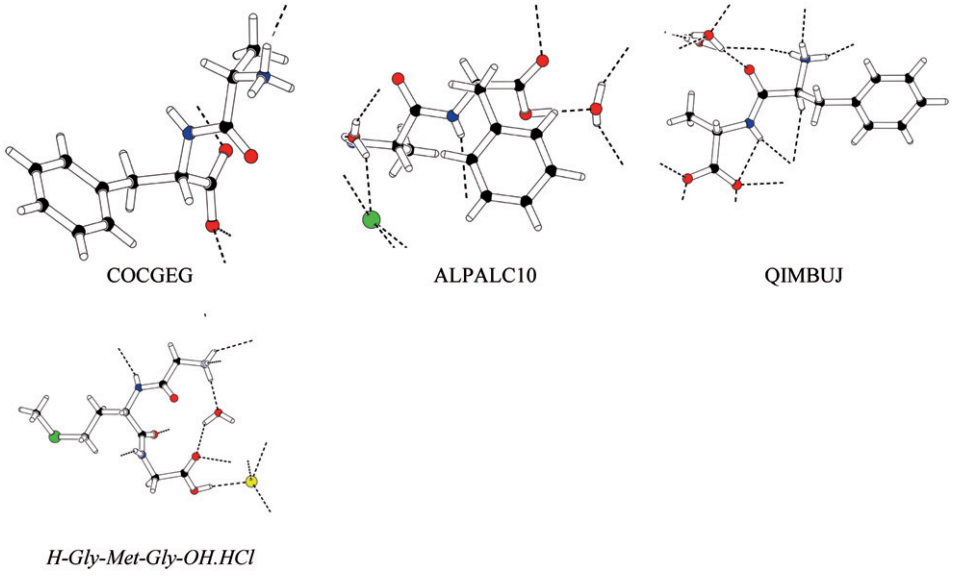

Figure 2. Hydrogen-bonding scheme in *H–Ala–Phe–OH* (COCGEG), *H–Ala–Phe–OH·HCl* (ALPALC10), *H–Phe–Ala–OH* (QIMBUJ), and *H–Gly–Met–Gly–OH·HCl* [93], given by the CCDC code (http://www.ccdc.cam.ac.uk/).

trans–O=C–NH fragment. Bands at 1675 and 1623 cm^{-1} are assigned to δ^{as}_{NH3+} and δ^{s}_{NH3+}, while the intense band at 1581 cm^{-1} to $\nu^{as}_{COO^-}$. These bands were overlapped by the maxima at 1600–1450 cm^{-1}, typical for i.p. vibrations of *In* ring. Only the band at 1469 cm^{-1} was well-defined. The intense band at 1396 cm^{-1} was attributed to $\nu^{s}_{COO^-}$. The theoretically approximated model of the system dipeptide/water revealed a torsion angle of 179.3(6)° for O=C–NH, i.e. a *transoid*-fragment.

2.1.2. Characterization by single crystal X-ray diffraction. Commonly, the characteristic IR and Raman bands (tables 1 and 2) strongly depend on the hydrogen-bonding schemes in the solid state. As a rule the stretching vibrations low-frequency shift with formation of the given hydrogen bond in solid state, in contrast to bending vibrations shifting to corresponding higher frequencies. Correlating the hydrogen-bonding scheme in solid state and the vibrational properties, summarized in tables 1 and 2, the common tendencies could be easily illustrated. The salt of *H–(Gly)$_2$–OH* showed the series of interactions in solid state $N^+H_3\cdots O/Cl$ (2.939, 2.749, 3.194, 3.188 Å) and $NH\cdots O$ (3.294 Å). The tripeptide *H–(Gly)$_3$–OH* was characterized with the same type of hydrogen bonds, i.e. $N^+H_3\cdots O$ (2.733, 2.749, 2.788, 2.913, 2.939 Å) and $NH\cdots O$ (2.920, 2.990 Å), similar to the corresponding hydrochloride ($N^+H_3\cdots O/Cl$ (3.256, 3.252, 3.220, 2.883 Å) and $NH\cdots O$ (2.956 Å)) as depicted in figure 1. The type of interaction was in accord with the observed vibrational characteristics shown in tables 1 and 2. A parallel study on the crystallographic and solid-state vibrational data of *H–Ala–Phe–OH* and its hydrochloride showed that the first compound had a series of hydrogen bonds, thus forming a 3-D network (figure 2): $N^+H_3\cdots O$ (2.761, 2.864, 2.897, and 3.029 Å), as well as $NH\cdots O$ (2.945 Å) bond between the amide NH and the

COO^--fragment. The corresponding interactions in the solid state of the salt were $N^+H_3 \cdots O$ (2.700, 2.776, 2.932 Å) and $NH \cdots O$ (3.017 Å), respectively. The weaker $NH \cdots O$ bond in the salt effect on the ν_{NH} vibration (table 1) was observed at higher frequencies by 11 cm^{-1}. The common tendency is valid as well for δ^{as}_{NH3+} observed at lower frequency in the neutral dipeptide, when the corresponding value of the hydrochloride salt is compared. The crystallographic data of *H–Phe–Ala–OH* (figure 2) showed the same type of interactions with bond distances of $N^+H_3 \cdots O$ (2.711, 2.788, 2.844 Å) and $NH \cdots O$ (2.984 Å), thus keeping the common tendencies for shift of the vibrational maxima in the solid-state spectra [174–195].

2.1.3. Characterization by nuclear magnetic resonance methods. The magnetic resonance investigations presented in our examination of peptide systems constituted a powerful method for structural determination of SP derivatives. Moreover, the ^{1}H- and ^{13}C-NMR characteristics of simple AA residues and SP have long been the subject of intense study, and many systematic and careful assignments of the chemical shifts are summarized in review articles, papers, and books [170–173, 178, 179, 196–200].

The data obtained for neutral *Gly*-containing peptides correlated well with analogous systems. The chemical shifts were practically unaffected after protonation of COO^- compared with corresponding zwitterionic tripeptides with exception of the proton signals of the groups directly attached to –COOH. In the case of *H–(Gly)$_3$–OH.HSq* the greatest chemical shift difference ($\Delta\delta$) was 0.64 ppm for the $\mathbf{CH_2}$-α_{gly3} signal. In other hydrogen squarates the important changes were 2.63 and 2.58 ppm for $\mathbf{CH_2}$-β_{met} and $\mathbf{CH_2}$-α_{gly1} in *H–(Gly)$_2$–Met–OH.HSq* and *H–Met–(Gly)$_2$–OH.HSq*, respectively.

The ^{13}C-NMR data of hydrogen squarates (*HSq*) differed significantly from those of the neutral DP, mainly in the appearance of four new signals at 170.00–184.47 ppm, associated with the HSq^- typical for *HSq* fragments. The other differences in the chemical shifts in ^{13}C-NMR spectra were connected to the directly protonated COO^- group in the pure peptides. For *H–(Gly)$_2$–OH.HSq*, *H–(Gly)$_2$–Met–OH.HSq*, and *H–Met–(Gly)$_2$–OH.HSq* the values of $\Delta\delta$ were 4.76 (**CO**-gly$_3$), 5.55 (**CO**-met) and 11.28 (**CO**-gly$_1$), respectively.

H–Gly–Ala–OH showed $\mathbf{CH_2}$ (*Gly*), **CH** (*Ala*) and $\mathbf{CH_3}$ (*Ala*) signals at 3.840, 4.443 ppm and a doublet at 1.425 and 1.446 ppm, respectively (the signal for **CH** (*Ala*) was observed as a quartet). The *Ala*-side chain signals in *H–(Ala)$_2$–OH* were observed at 4.446 (**CH**), 1.430 and 1.444 ($\mathbf{CH_3}$) ppm. As compared to the corresponding zwitterions, with exception of the proton signals of the groups directly attached to –COOH, the chemical shifts in the ^{1}H NMR spectra were practically uninfluenced on protonation of $-COO^-$. In the salts, the significant chemical shift differences ($\Delta\delta$) were 0.50 and 0.62 ppm for –**CH** (*Ala*) signals. The ^{13}C-NMR data for *HSqs* showed four signals in the chemical shift range of 169.9–184.6 ppm (about 186.0, 172.0, 171.0, and 169.0 ppm). The other differences in the chemical shifts of the ^{13}C-NMR spectra were associated with protonated $-COO^-$ in pure peptides. The **CO**-values for the salts of *H–Gly–Ala–OH* and *H–(Ala)$_2$–OH* are $\Delta\delta = 6.76$ and 5.70 ppm, while those for the neutral forms are 174.8 and 171.7 ppm, respectively.

2.1.4. Characterization by electrospray ionization-mass spectrometry. Electrospray ionization-mass spectrometry (ESI-MS) both in single (MS) and tandem (MS/MS) mode readily yielded molecular weights together with structural information [180–190].

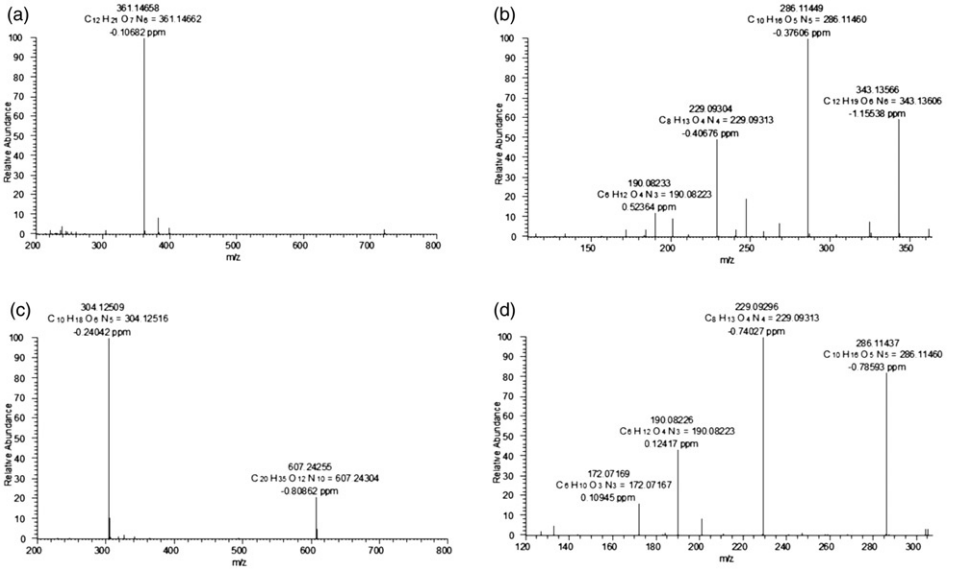

Figure 3. High resolution ESI-MS and ESI-MS/MS spectra of *H–(Gly)$_5$–OH* (A, B), *H–(Gly)$_6$–OH* (C, D).

The state of the art of high resolution mass spectrometers like the Thermo Fisher Orbitrap includes high mass resolution (up to 100,000), large space charge capacity, high mass accuracy (2–5 ppm), a mass/charge range of at least 6000, and dynamic range greater than 10^3 [201]. It is the method of choice for analysis of SP and their metal complexes because sensitivity and selectivity has been demonstrated for small *Gly* homopeptides and some of their Cu^{II} and Ag^{III} complexes. The high resolution spectrum of *H–(Gly)$_6$–OH* was characterized by a peak at *m/z* 361.14658, corresponding to a singly charged cation $[C_{12}H_{21}O_7N_6]^+$ with a calculated molecular weight of 361.14662 (figure 3). The ESI-MS/MS spectrum of *H–(Gly)$_6$–OH* was characterized by fragments after loss of H_2O (*m/z* 343.13566; $[C_{12}H_{19}O_6N_6]^+$) and complete glycine groups (*m/z* 286.11449; $[C_{10}H_{16}O_5N_5]^+$). The ESI-MS spectrum of *H–(Gly)$_5$–OH.HSq* was characterized by a peak at *m/z* 304.12509 $[C_{10}H_{18}O_6N_5]^+$ and a second signal at *m/z* 607.24255 $[C_{20}H_{35}O_{12}N_{10}]^+$ which was associated with its dimer. According to our studies on humic and fulvic acids, where the preferred ionization in the positive mode for the amines was observed [185, 187, 188, 190], it would be expected that the NH_3^+ derivatives of the peptides would be formed in the gas phase [191]. If fragmentation of *H–(Gly)$_5$–OH* and *H–(Gly)$_6$–OH* followed the common scheme for SP [191], we should have observed peaks without a *Gly*-molecule. In contrast, we observed a series of peaks at *m/z* 286.11 ($[C_{10}H_{16}O_5N_5]^+$), 229.09 ($[C_8H_{13}O_4N_4]^+$), and 190.08 ($[C_6H_{10}O_3N_3]^+$) which corresponded most probably to the cyclic penta-, tetra-, and tripeptides.

2.2. *Theoretical characterization*

Protonation of the COO-group in *H–(Gly)$_2$–OH* led to deviation of the absolute planarity in the neutral form of 13.5(0)°. In the case of the tripeptide the value was 12.7(2)° (table 3). The protonation or coordination led to a distortion of the

Table 3. Experimental crystallographic data for dihedral angles of amide O=C–NH group (°) of *H–(Gly)$_2$–OH*, *H–(Gly)$_3$–OH*, and their derivatives as well as the angle between the amide planes in the tripeptides. The compounds are given with the corresponding CCDC codes.

Dipeptides		Tripeptides			
			O=C–NH angle (°)		Angle between the amide planes (°)
CCDC code	O=C–NH angle (°)	CCDC code	*gly$_1$*	*gly$_2$*	
GLYGLY [114]	**178.7(0)**	GLYLIB [116]	176.4(6)	157.3(7)	75.5(5)
POTPET [115]	173.5(0)	TGLYCY [132]	**173.7(9)**	**178.2(6)**	**9.9(1)**
GLCICH [116]	170.4(5)	GGGCAC [133]	170.0(4)	171.8(2)	85.4(1)
GLGLYN10 [128]	179.7(0)	BIBRUZ [134]	**161.0(5)**	**173.7(2)**	**28.4(4)**
GLYGLP [129]	**165.6(5)**	ZEXRAV [135]	*171.5(5)*	*179.2(8)*	*12.1(9)*
HIBBID [130]	176.9(3)	–	–	–	–
HIBBIP [130]	174.5(3)	–	–	–	–
MUNQER [131]	176.1(5)	–	–	–	–

co-planarity of the two amide fragments which may vary between 9.9(1)° and 85.4(1)°, depending on the type of the counterion or specific interactions with the metal ion. The vibrational characteristics of the amide fragments of *H-(Gly)$_3$–OH* and its salts [18–39] were found with ν_{NH} and amide I vibrations at 3313, 3298, 1657, and 1646 cm^{-1}. The *trans*- and co-planar dispositions of both amide fragments were experimentally verified by single-crystal X-ray diffraction data (175.6°, 177.7°, and 0.1°, respectively) [117]. The crystallographic data of the salt defined a *transoid*–C(=O)–NH and angles of 161.0° and 173.2° [118], resulting in bands at 3313, 3280, 1678, and 1656 cm^{-1} (table 1). The elucidation of vibrations of the higher analogs of the *Gly*-homopeptides revealed the same tendencies for the shift in characteristic vibrational bands as a result of protonation.

Theoretical analysis of the higher *Met*-containing analogs showed a series of conformers with energy less than 5 kJ mol^{-1}: *H–(Gly)$_2$–Met–OH* (0.0 kJ mol^{-1}) and *H–Met–(Gly)$_2$–OH* (0.1 kJ mol^{-1}). A planar disposition of both amide fragments was assumed in *H–Met–(Gly)$_2$–OH*, determining a co-linear disposition of *gly$_1$* and *gly$_2$* amide I and ν_{NH} transition moments. However, a deviation of 24.2° in *H–(Gly)$_2$–Met–OH* in the amide fragments was theoretically established. The optimized geometry parameters agreed reasonably well with those refined by crystallographic data for other tripeptides with *Gly*- and *Met*-residues [166–169]. The experimental and theoretical data for atomic distances and angles did not differ by more than 0.012 Å and 2.3(5)°, respectively [166–169]. Analysis of *H–Gly–Met–Gly–OH* and *H–Gly–Met–Gly–OH.HCl* revealed most stable conformers with minimum energy of 0.1 and 0.2 kJ mol^{-1}. The optimized structural parameters for both systems are in agreement with crystallographic data for *H–Gly–Met–Gly–OH* and *H–Gly–Met–Gly–OH.HCl* (C–O bond lengths in –COO$^-$ group of 1.240 Å (C=O) and 1.320 Å (C–OH), respectively). The ν_{NH} peaks for the amide fragments were observed at 3343 and 3309 cm^{-1}. The 1700–1450 cm^{-1} region revealed an intense positive peak at 1660 and 1643 cm^{-1} belonging to amide I vibrations. The crystallographic data confirmed the protonation of the COOH fragment and retention of a protonated –NH_3^+ group. The bond lengths and angles are similar to those of other *Met*-containing di- and tripeptides [166–169]. The data confirmed the *trans*–C(=O)–NH fragments with dihedral angles of 176.01° and 173.14°.

Protonation of the carboxylate led to inequality of the C–O bond lengths with the formation of effectively double C=O (1.196 Å) and single C–O bonds (1.322 Å). Three types of intermolecular interactions were also established: gly_1 NH $\cdots$ Cl, $NH_3^+ \cdots OH_2$, and (COO)H $\cdots$ Cl (2.383, 2.461, and 2.216 Å, respectively) (figure 2). Thus, formation of hydrogen bonds with water created a dihedral angle at 42.34° between the planes of the gly_1 and gly_2 amide groups.

The calculations identified a series of conformational minima for both *H–(Ala)$_2$–OH* and *H–Gly–Ala–OH*. Of those with energy below 5.0 kcal mol^{-1}, there were five for *H–(Ala)$_2$–OH* and its protonated form and six for protonated *H–Gly–Ala–OH*. Since the conformations play a crucial role in biological activity of peptides and their derivatives, a precise conformational analysis of these was performed by minimization of energy and optimization of dihedral angles.

Backbone conformations with intramolecular $N^+H_3 \cdots O{=}C{-}NH_2$ bonds were more stable than structures with bifurcated N^+H_3 to C=O interactions (2.743–2.785 Å). The former bond is a conventional interaction, commonly accepted to play the dominant role in the relative stability of the conformation. The most stable conformers were characterized with energy 0.0 kcal mol^{-1} (*H-(Ala)$_2$–OH*), 0.6 kcal mol^{-1} (protonated *H–(Ala)$_2$–OH*) and 1.1 kcal mol^{-1} (protonated *H–Gly–Ala–OH*). The results assumed *transoid*-amide fragments with torsion angle CO–NH of 174.1° in *H-(Ala)$_2$–OH* (table 3). Comparing both crystallographic [170] and theoretical geometry parameters as atomic distances and angles, a good correlation was established as the values did not differ by more than 0.064 Å and 9.7(5)°. The experimental data indicated a *trans*–CO–NH fragment (173.4°) and an NCC(O)N(H) angle of 165.4°. The protonation of *H–(Ala)$_2$–OH* led to a *transoid*–CO–NH group (165.8°). The experimental value for the hydrochloride was 163.4°. Protonation affected other dihedral angles as well. The theoretical data of NH–CC(OO), NCCO(O), and NCC(O)N(H) are 119.5°, 120.0°, and 169.4°, respectively, while the corresponding experimental ones are 47.8°, 162.7°, and 156.9°. Other geometric parameters did not differ by more than 0.014 Å and 6.9(3)° [173]. A similar tendency was also established for *H–Gly–Ala–OH*. The predicted geometric parameters correlated well with experimental data for the hydrochloride salt, where the atomic distances and angles did not differ by more than 0.093 Å and 8.8(6)°, respectively. It is interesting to note that the experimentally observed conformation of the protonated form of a given peptide depends on the type of anionic fragment and the presence of solvent, leading to the possibility for differences according to type and strong intra- or intermolecular interactions [196–200]. In *H–(Ala)$_2$–OH* hydrochloride the CO–NH, NH–CC(OO), NCCO(O), and NCC(O)N(H) angles were 173.4°, 70.9°, 76.7°, and 165.4°, while for 1,5-naphthalenedisulfonate salt the values were 169.4°, 102.3°, 150.8°, and 163.9°, respectively [200].

The neutral and protonated forms of *H–Thr–Ser–OH* were characterized with most stable conformers having energy of 0.6 and 0.4 kJ mol^{-1} as well as *trans*- and *transoid*-amide fragments of 177.3(6)° and 171.8(5)°, respectively. The optimized structural parameters are in good agreement with crystallographic data for *Thr*- and *Ser*-containing peptides such as *H–Ala–Thr–OH*, *H–Gly–Thr–OH*, or *H–Ser–Leu–OH* with N(H)–C(=O) angles of 173.9°, 174.3°, and 177.8°, respectively [202–205]. The salts showed parameters for COO^- of 1.200 Å (C=O) and 1.277 Å (C–OH).

The data indicated a *trans*-amide fragment. The most stable conformers of *H–Phe–Tyr–OH* and its protonated form were characterized with minimum energy of 0.0 kJ mol^{-1}. Protonation did not exert any effect on the observed *trans*-amide

fragments with dihedral angles at 177.5° and 178.4° for *H–Phe–Tyr–OH* and its salt. The optimized values of the geometric parameters agreed reasonably well with those obtained by crystallographic data for similar *Phe*-residues, where both the experimental and theoretical results for atomic distances and angles did not differ by more than 0.012 Å and 0.1(1)° [205, 206].

H–Tyr–Trp–OH was also analyzed theoretically, yielding structural parameters corresponding to minimum energy of 0.1 kJ mol^{-1}. This correlated well with the known crystallographic results for other dipeptides [207–213]. The theoretically predicted and experimentally determined parameters, bond lengths and angles ranged between 0.005–0.012 Å and 0.2°–0.5°, respectively. The amide fragment was *trans*-flat with a torsion angle of 175.9°. Both the skeletons of aromatic phenyl and indole (*In*) fragments possessed a nearly co-planar disposition with an angle of 7.8°. The *In* ring was almost planar with a dihedral angle deviation of 1.2°–5.4°, while the NH group was in the frame of the *In* plane with a deviation of 0.4°. The *Tyr*-aromatic skeleton was planar with calculated dihedral angles between 0.5° and 1.3°.

From the IR-data and the known crystal structure, *H–Gly–Trp–OH·2H$_2$O* was characterized [214]. The flat *trans*-configurated HN–C=O fragment (177.4(9)°) [210] (figure 2) was characterized with typical values of characteristic vibrations (table 1). Isolation and crystallographic characterization of the corresponding Cu^{II}–complexes permitted a parallel study of the spectroscopic and structural changes during coordination. The ligand participated in tridentate chelation through –NH$_2$, N$_{-1}$, and –COO$^-$ binding sides, fusing five- and six-membered chelate rings. Complexes of *H–Gly–Trp–OH* as well as *H–Trp–Gly–OH* with M^{II} metal ions such as Cu^{II}, Co^{II}, Ni^{II} have distinct properties [212–215]. The binding of the metal ion was strongly influenced by the AA sequence and pH.

3. Coordination ability of SP

3.1. *Experimental characterization*

3.1.1. Characterization by vibrational (IR and Raman) spectroscopy. As mentioned above for the amide fragments the typical vibrational bands may provide information concerning the peptides' manner of coordination [18–39, 87–107, 216–222]. Monodentate coordination of the peptides through COO$^-$ (figure 4(I)) leads to the

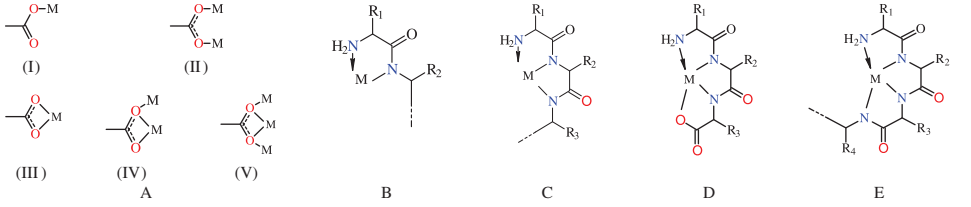

Figure 4. The mode of coordination of –COO$^-$ in the zwitterionic peptides (A); coordination chelating modes through –NH$_2$– and –N$_{-1}$ (amide) centers from the N-termini (B), (C), and (E) and tetradentate coordination through –NH$_2$–, 2 –N$_{-1}$ (amide fragments) and O-(C=O) centers.

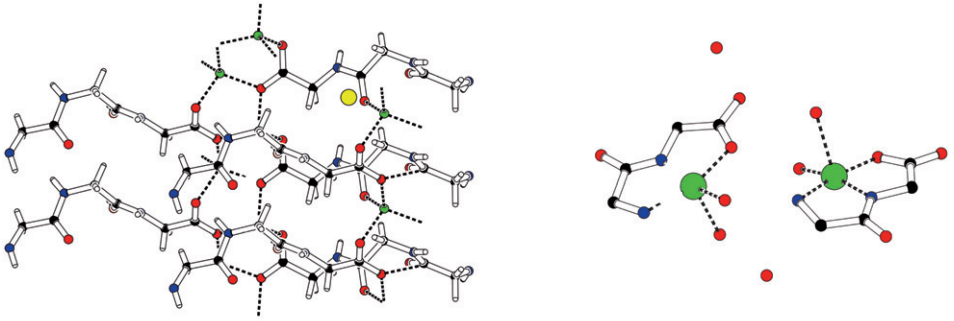

Figure 5. Crystallographic data for *H–(Gly)$_2$–OH* lithium bromide (GLYLIB) [116]; and corresponding Cu(II) complex (CGLGLT) [117]. The crystal structures are given by their CCDC codes (http://www.ccdc.cam.ac.uk/).

formation of a COOH group. However, the corresponding band was low-frequency shifted by about 50 cm^{-1}. Symmetric bidentate interactions, that is figure 4(II), (III), and (V) led to the observation of $\nu^{as}_{COO^-}$ and $\nu^{s}_{COO^-}$ like those in the free peptides; however, shifting of up to 20 cm^{-1} to lower frequency was observed [18–39, 87–107]. Raman spectroscopy is predominantly a method for elucidation of aliphatic peptides, thus giving a relatively "sparse" pattern without strong overlapping effects, while aromatic peptides, especially those containing *Trp* as AA residue, often are characterized with a fluorescence band and consequently the application of the method is limited. In accordance with theory, the ν^{as}_{NH3+} and δ^{as}_{NH3+} stretching and bending vibrations of NH_3^+ in each of the zwitterionic peptides are low-frequency absorptions positioned less than 2 cm^{-1} from the corresponding IR bands. The same applied to amide I vibrations. Coordination through the amino group (figure 4(B)–(E)) led to the disappearance of IR bands for NH_3^+ and observation of the ν^{as}_{NH2} and ν^{s}_{NH2} maxima at 3500–3000 cm^{-1} as well as δ_{NH2} about 1650–1690 cm^{-1} as a XY_2-local symmetry system [112, 113]. The stretching vibrations were low-frequency shifted by about 100 cm^{-1}, from typical NH_2-group values [18–39, 87–107, 112] (table 2).

3.1.2. Characterization by single-crystal X-ray diffraction. Spectroscopic characteristics of the metal complexes of peptides change dramatically during complexation. Typically dipeptides participate in tridentate chelation by the N-terminal AA residue, through the NH_2, N_{-1}, OCO^--fragments, as was obtained in Cu^{II} and Pt^{II} complexes [114–118]. These binding sites were fused in five- and six-membered chelate rings (figures 5 and 6). Interaction of *H–(Gly)$_2$–OH* with Pt^{II} led to the formation of mononuclear complexes with bidentate coordination (figure 4(B) and figure 5) as potassium dichloro–((*Gly*)$_2$–N,N′)–Pt^{II} (NOJKUS) and dichloro-((*Gly*)$_2$–N,N′)–Pt^{II} dihydrate (NOJLAZ) [119]. Depending on the reaction conditions *H-(Gly)$_2$–OH* could interact tridentately through NH_2, N_{-1}, and OCO^--centers, as observed in the potassium ((*Gly*)$_2$–trichloro–Pt^{IV} monohydrate (XEVYIG) [120] (figure 5) or ammonium *bis*((*Gly*)$_2$–N,N′,O)–Co^{III} dihydrate (AGGLCO) [121]. It is interesting to note that *H–(Gly)$_2$–OH* is mono- or bidentate through the COO^--group (figure 4(I), (II)) in tetrasodium *bis*((*Gly*)$_2$-γ-octamolybdate pentadecahydrate (LECSAO) [122],

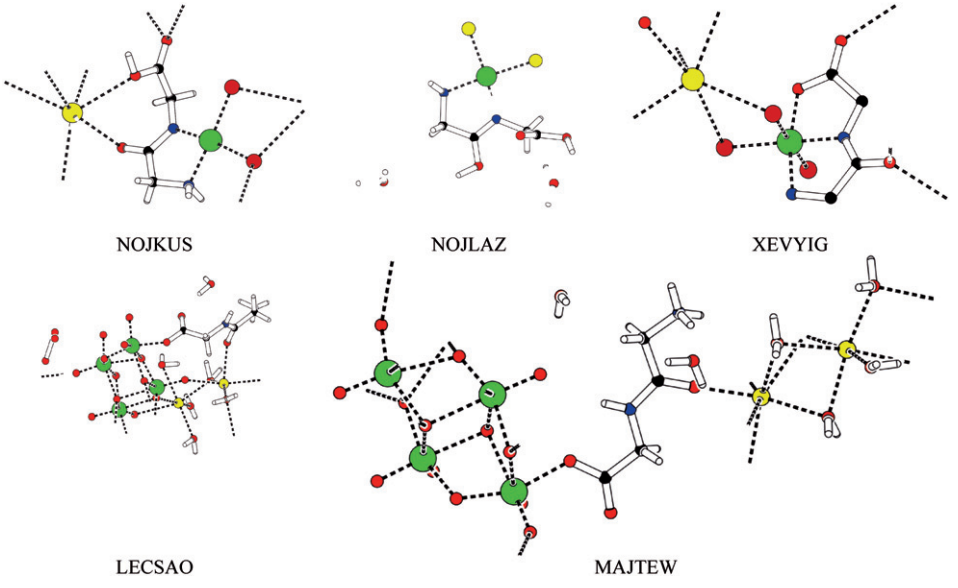

Figure 6. Crystal structure of metal complexes with *H–(Gly)$_2$–OH* [119–124]. The crystal structures are given by their CCDC codes (http://www.ccdc.cam.ac.uk/).

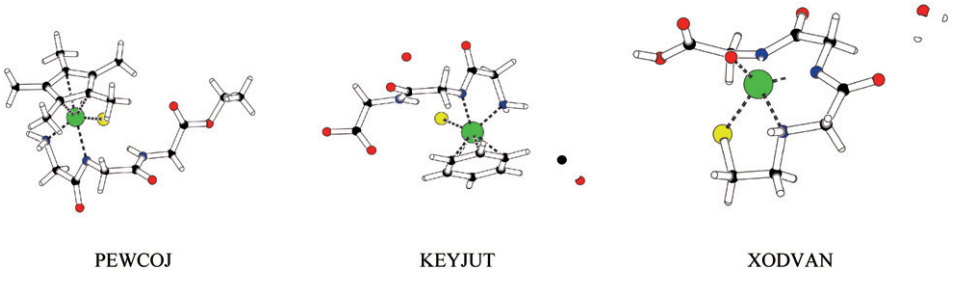

Figure 7. Crystal structures of the metal complexes with CCDC codes PEWCOJ, KEYJUT) and XODVAN, respectively [124–126]. The crystal structures are given by their CCDC codes (http://www.ccdc.cam.ac.uk/).

tetrasodium *bis*((*Gly*)$_2$-hexacosaoxo-octa-Mo^{VI} dodecahydrate (MAJTEW) [123], or (*Gly*)$_2$-Ag^{I} nitrate (GGAGNI) [124] (figures 6 and 7).

The tripeptides often are tetradentate ligands with metal ions such as Cu^{II} or Pt^{II}, forming a chelate through –NH$_2$, 2N$_{-1}$, and –OCO^{-}-centers (figure 4D). Depending on the pH of the medium, the coordination mode can be any of those depicted in figure 4(B)–(E). Like dipeptides, tripeptides may also be bidentate through the –NH$_2$, N$_{-1}$ centers (figure 4B) in the (chloro-(η^5-pentamethyl-cyclopentadienyl)-((*Gly*)$_3$-ethyl-ester-N,N′))-Rh^{I} (PEWCOJ) [125] or chloro-(η^6-benzene)-(*tri-Gly*-N,N′)–Ru^{II} monohydrate methanol solvate (KEYJUT) [126], figure 6. In (N-mercaptoethyl-(*Gly*)$_3$)-oxo-Re^{II} monohydrate (XODVAN) [126], the ligand is tetradentate through S and 3N$_{-1}$ centers (figure 4C).

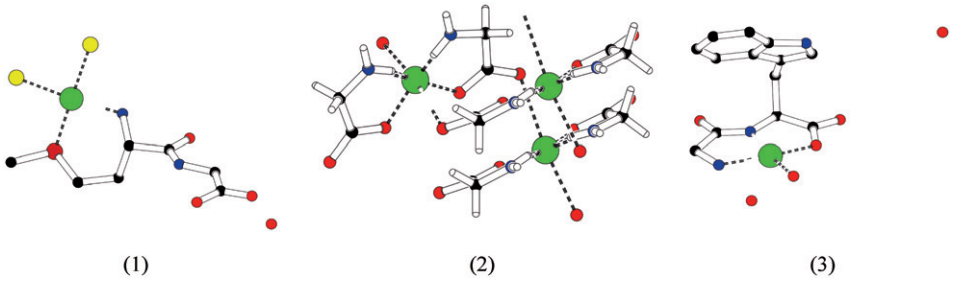

Figure 8. PLUTON diagram of the Pt^{II} complex of *H–Met–Gly–OH* [172] (1), *bis(glycinato)*Cu^{II} complex (2) and (glycyltryptophane)Cu^{II} (3) [216].

The data for higher *Gly*-analogs revealed that the values for δ_{NH} are typical of *trans*-amide fragments where the frequency of the IR band corresponding to δ_{NH} was observed at 1560–1530 cm^{-1} (table 1). However, strong overlapping of the spectroscopic patterns required application of other physical methods, such as NMR and MS, for analysis. In parallel to the experimental study, the theoretical approaches for predicting molecular geometry and physical properties of these complicated systems were also successfully employed, thus making their complete characterization possible [136–169]. The *Ala*-residue exerted a weak effect on the basic vibrations (table 2) at 1640 cm^{-1} (*H–Gly–Ala–OH*) and at 1670 cm^{-1} (*H–Gly–(Ala)$_2$–OH*) for the bending vibrations of NH_3^+, at 3200 cm^{-1} (ν_{NH}), 1690–1640 cm^{-1} region ($\nu_{C=O}$) and about 1560 cm^{-1} (δ_{NH}). The $\nu^{as}_{COO^-}$ and $\nu^{s}_{COO^-}$ were observed within the 1590–1560 cm^{-1} region and at 1420 cm^{-1}.

Crystallographic data for the coordination ability of the *H–Gly–Ala–H* analog have been described as tridentate through NH_2, N_{-1}, and OCO^- centers in the corresponding K[Pt(*Gly–β–Ala–OH*)Cl]. This is in contrast to [Pt(*Gly–His*)Cl], where the coordination mode is also tridentate through 3N centers [40]. In contrast to *Gly*-containing peptides, in *Met*-containing derivatives the coordination of the thioether S-donor group is predominant [40, 74–76, 88, 97, 169, 174–176] as described in [Pt(*H–Met–Gly–OH*)Cl_2] (figure 8). The interaction of Cu^{II} with H–(*Gly*)$_2$–OH led to formation of the metal complex with a signal at *m/z* 211.98 (figure 9, Table 4, $[C_4H_9O_4N_2Cu]^+$); that is a formation of a *bis*(*glycinato*)Cu^{II} complex with possible *cis*- and *trans*-isomerization [214–216]. However, the formation of such type of complex with *H–(Gly)$_2$–OH* proposed a peptide bond cleavage under the reaction conditions.

The interaction of *H–Gly–Trp–OH* with Cu^{II} led to the formation of the mononuclear complex (figure 8) [216–218] with a tridentate coordination of the ligand through $–NH_2$, N_{-1}, and OCO^-. In contrast to protonation, the complexation of the peptide led to a drastic conformational change of the peptide molecule. On comparison of the crystallographic data for the zwitterionic peptide and its metal complex [211, 213], it revealed that the main effect is on the NH–CC(OO) and CNCCO(O) angles with differences of 66.2(5)° and 55.4(9)°. The distance between the *In* skeleton and the Cu^{II} center of 4.246 Å highlights to the π-stacking effect as described [1–4].

3.1.3. Characterization by ESI-MS. To elucidate the type of binding of metal complexes the MS data obtained have been correlated with the single-crystal X-ray

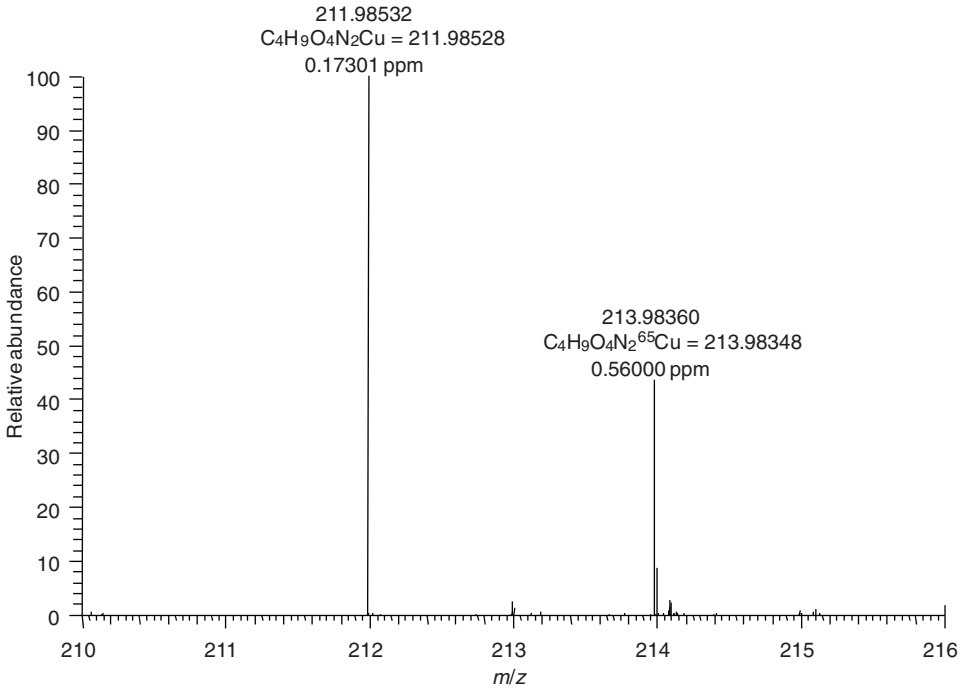

Figure 9. High resolution ESI-MS spectrum of *bis*(glycinato)Cu^{II} complex.

Table 4. Crystallographic and refinement data for *bis(glycinato)*Cu^{II} complex.

Empirical formula	$C_4H_8N_2O_5$
Formula weight	227.66
Temperature (K)	206(2)
Wavelength λ (Å)	0.71073
Crystal system	Orthorhombic
Space group	$P2_12_12_1$
Unit cell dimensions (Å, °)	
a	5.229(3)
b	10.824(7)
c	13.514(9)
α	90
β	90
γ	90
Volume (Å^3), *Z*	764.9(8), 4
Calculated density ρ_{calc} (Mg m^{-3})	1.977
Absorption coefficient, μ (mm^{-1})	2.841
Crystal size (mm^3)	$0.53 \times 0.28 \times 0.22$
Goodness-of-fit on F^2	1.066
R_1 [$I > 2\sigma(I)$]	0.0755

diffraction data (figure 8). Crystallization in the non-centrosymmetric orthorhombic $P2_12_12_1$ space group makes the *cis*-isomer a candidate for metal–organic material with NLO properties in the bulk. The geometry of the $Cu^{II}N_2O_4$ chromophore can be described as perturbed O_h with the Cu–O and Cu–N distances of 2.030, 1.952, 1.969 Å

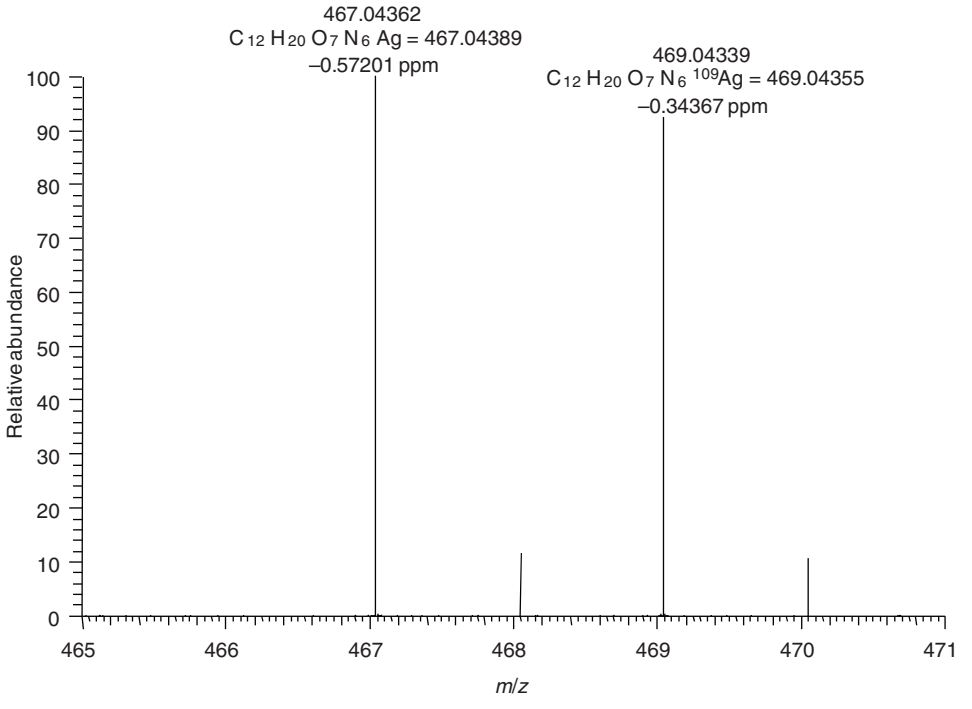

Figure 10. High resolution ESI-MS spectrum of Ag(III) complex of *H*–(*Gly*)$_6$–*OH*.

with O–Cu–O and N–Cu–O angles within the range 83.8(6)°–95.7(8)°. The analysis by high resolution ESI-MS exhibited a quasi-molecular ion with formula $C_4H_9O_4Cu$, indicating a "covalent?" bound copper to the organic moiety. This result is supported by the characteristic isotopic pattern of the observed mass peaks, which exhibited the natural distribution of copper 63 and 65 in a ratio of 69/30. Another example that MS is a powerful tool for the analysis of this type of compounds entails the high resolution ESI-MS spectrum of the Ag^{III}-complex of *H*-(*Gly*)$_6$-*OH* where two peaks at *m*/*z* 467.04365 ($[C_{12}H_{20}O_7N_6^{107}Ag]^+$) and 469.04343 ($[C_{12}H_{20}O_7N_6^{109}Ag]^+$) were exhibited and in good agreement with the calculated sum formulae for the two silver isotopes 107 and 109, additionally showing the correct isotopic distribution of silver (52/48) (figure 10). Most probably the detected ions corresponded to a mononuclear Ag^{III} peptide complex, stable in the gas phase according to classical tetradentate coordination figure 4(E).

3.2. *Theoretical characterization*

During optimization of the molecular geometry of the peptides and their metal complexes by *ab initio* and DFT methods, frequency calculations, predicting optical, and NLO properties and/or studies of specific interactions are the common approaches for the application of theoretical methods [10, 13, 15, 16, 222–233]. Theoretical characterization of the conformational changes of the peptides as a result of coordination with the metal ions is important because their activity depends not only

on the metal ion, but also on the way the molecule is folded, and in many cases conformational changes appear to be prerequisites. In our studies, for conformation and optical properties, we used mainly the DFT or hybrid methods [231, 232]. Similar to other studies [222–229], it has been found that partial or full geometry optimization is essential in most cases for the determination of structures, since the experimental conformations rarely give the precise theoretical minimum. Especially for comparison between the gas- and condensed-phase parameters it has been found that for the obtained geometry parameters such as bond lengths and angles for both neutral or protonated peptides and their metal complexes, the theoretical mode makes valuable (in some cases excellent) contributions between the structural-theoretic and/or structural/spectroscopic approaches. In contrast, the dihedral angles strongly depend on the inter- and/or intramolecular interactions.

4. Conclusion and outlook

In this review, we have outlined possible strategies toward elucidation of the coordination and protonation ability of SP, including theoretical approaches and physical measurements. The coordination chemistry of peptide systems is a powerful tool for designing novel biologically active compounds with tunable physiological effects, based on the properties of the essential metal included as well as on the design of novel drugs with anticancer activity.

Perhaps most importantly, it is essential to introduce new perspectives for coordination compounds of SP, that is their possible application as novel NLO materials [25, 30–33, 37, 38]. Although the 3-D structures of peptides and their derivatives have been determined over the past decades, their crystallization is still a major obstacle to crystallographic work. The presence of chiral center/s adds further difficulties. However, for such a class of novel NLO materials, metal–organic coordination networks with peptides should yield non-centrosymmetric solids based on 1-D to 3-D related helical networks, depending on the optical properties of the metal ions, the type of the amino-acid residues, a favorable combination of thermal and chemical stability, solubility characteristics, transparency, and second-order optical non-linearity, that is potential candidates for applications in electro-optic devices. Logically, the question arises, what is next. There is large potential for further molecular-level studies on the coordination and protonation ability of selected SP with metal ions with a view to designing their crystallization networks and supramolecular properties, with an overall aim of optimizing the NLO properties and further investigating the possibilities for switching optical behavior using such compounds.

Supplementary material

Crystallographic data for the structural analysis have been deposited with the Cambridge Crystallographic Data Centre, CCDC 795568. Copies of this information may be obtained from the Director, CCDC, 12 Union Road, Cambridge, CB2 1EZ, UK (Fax: +44 1223 336 033; E-mail: deposit@ccdc.cam.ac.uk or http://www.ccdc.cam.ac.uk).

Acknowledgments

The authors thank the *DAAD*-Deutscher Akademischer Austausch Dienst for a grant within the priority program "Stability Pact South-Eastern Europe" and the DFG-Deutsche Forschungsgemeinschaft for Grants SPP 255/21-1 and SPP/22-1. The authors also thank the central instrumental laboratories for structural analysis at TU Dortmund University of Technology (Germany) and the analytical and computational laboratories at the Institute of Environmental Research (INFU) at the TU Dortmund (Germany) as well as express their gratitude to all researchers who contributed actively to the development of the discussed research field within the framework of DAAD and DFG.

References

[1] J. Sunner, K. Nashizawa, P. Kebarle. *J. Phys. Chem.*, **85**, 1814 (1981).
[2] D. Dougherty. *Science*, **271**, 163 (1996).
[3] J. Ma, D. Dougherty. *Chem. Rev.*, **97**, 1303 (1997).
[4] R. Kumpf, D. Dougherty. *Science*, **261**, 1708 (1993).
[5] K. Scheller, K. Hofstetter, P. Mitchell, P. Prijs, H. Sigel. *J. Am. Chem. Soc.*, **102**, 247 (1981).
[6] H. Siegel. In *Advances in Solution Chemistry*, I. Bertini, L. Lunazzi, A. Dei (Eds), Plenum, NewYork (1981).
[7] H. Siegel. *Chimia*, **41**, 11 (1987).
[8] B. Fischer, H. Siegel. *J. Am. Chem. Soc.*, **102**, 2998 (1981).
[9] H. Siegel. *Pure Appl. Chem.*, **61**, 923 (1989).
[10] H. Siegel, H. Tribolet, O. Yamauchi. *Comments Inorg. Chem.*, **9**, 305 (1990).
[11] H. Siegel. *Inorg. Chem.*, **14**, 1535 (1975).
[12] H. Siegel, P. Martin. *Chem. Rev.*, **82**, 385 (1982).
[13] O. Yamauchi, O. Nakao, A. Nakahara. *Bull. Chem. Soc. Japan*, **48**, 2572 (1975).
[14] O. Yamauchi, A. Odani. *J. Am. Chem. Soc.*, **103**, 391 (1981).
[15] O. Yamauchi, A. Odani, H. Masuda. *Inorg. Chim. Acta*, **198**, 749 (1982).
[16] O. Yamauchi, A. Odani. *J. Am. Chem. Soc.*, **107**, 5938 (1985).
[17] C. Bosshard, J. Hulliger, M. Florsheimer, P. Günter. *Organic Nonlinear Optical Materials, Advances in Nonlinear Optics*, Gordon and Breach Science Publishers SA, Postfach, Basel (2001).
[18] D. Chemla, J. Zyss. In *Nonlinear Optical Properties of Organic Molecules and Crystals*, D. Chemla, J. Zyss (Eds), Vol. 1, Academic Press, New York (1987).
[19] H. Nalwa, T. Watanabe, S. Miyata. In *Nonlinear Optics of Organic Molecules and Polymers*, H. Nalwa, S. Miyata (Eds), CRC Press, Boca Raton, FL (1997).
[20] K. Sakada. *Optical Properties of Photonic Crystals*, Springer, Berlin (2005).
[21] J. Reetz, S. Hoger, K. Harris. *Angew. Chem. Int. Ed.*, **33**, 181 (1994).
[22] J. Zyss. In *Molecular Nonlinear Optics: Material Physics and Devices*, J. Zyss (Ed.), Academic Press Inc, San Diego (1993).
[23] V. Geskin, C. Lambert, J. Bredas. *J. Am. Chem. Soc.*, **125**, 15651 (2003).
[24] R. Wampler, A. Moad, C. Moad, R. Heiland, G. Simpson. *Acc. Chem. Res.*, **40**, 953 (2007).
[25] P. Sullivan, L. Dalton. *Acc. Chem. Res.*, **43**, 10 (2010).
[26] P. Brian. USA Patent, PCT/GB/91/00616 (1991).
[27] J. Wolff, R. Wortmann. *Adv. Phys. Org. Chem.*, **32**, 121 (1999).
[28] S. Neeraj, M. Noy, C. Rao, A. Cheetham. *Solid State Sci.*, **4**, 1231 (2002).
[29] C. Robl, A. Weiss. *Z. Anorg. Allg. Chem.*, **546**, 161 (1987).
[30] O. Evans, W. Lin. *Acc. Chem. Res.*, **35**, 511 (2002).
[31] T. Radhakrishnan. *Acc. Chem. Res.*, **41**, 367 (2008).
[32] B. Coe. *Acc. Chem. Res.*, **39**, 383 (2006).
[33] O. Maury, H. Le Bozec. *Acc. Chem. Res.*, **38**, 691 (2005).
[34] B. Ivanova, R. Seidel, T. Kolev, W. Sheldrick, M. Spiteller. *Amino Acids*, **39**, 309 (2010).
[35] B. Ivanova, M. Spiteller. *Biopolymers*, **39**, 724 (2010).
[36] T. Kolev, B. Koleva, M. Spiteller, W. Sheldrick, H. Mayer-Figge. *Amino Acids*, **36**, 185 (2009).
[37] T. Kolev, M. Spiteller, B. Koleva. *Amino Acids*, **38**, 45 (2010).
[38] K. Rieckhoff, W. Peticolas. *Science*, **147**, 610 (1965).
[39] B. Koleva, M. Spiteller, T. Kolev. *Amino Acids*, **38**, 295 (2010).

[40] E. Farkas, I. Sovago. *Amino Acids*, **33**, 295 (2002).
[41] N. Lomadze, H. Schneider. *Tetrahedron Lett*., **46**, 751 (2005).
[42] J.F. Stoddart. *Acc. Chem. Res*., **34**, 410 (2001).
[43] A. Balzani, F. Credi, F. Raymo, J.F. Stoddart. *Angew. Chem., Int. Ed*., **39**, 3349 (2000).
[44] A. Harada. *Acc. Chem. Res*., **34**, 456 (2001).
[45] J. Collin, C. Dietrich-Buchecker, P. Gavina, M. Jimenez-Molero, J. Sauvage. *Acc. Chem. Res*., **34**, 477 (2001).
[46] D. Robinson, N. Peppas. *Macromolecules*, **35**, 3668 (2002).
[47] H. Schneider, L. Tianjun, N. Lomadze. *Angew. Chem., Int. Ed*., **42**, 3544 (2003).
[48] J. Canary, B. Gibb. *Progr. Inorg. Chem*., **45**, 1 (1997).
[49] J. Steed. *Coord. Chem. Rev*., **215**, 171 (2001).
[50] M. Deetz, M. Shang, B. Smith. *J. Am. Chem. Soc*., **122**, 6201 (2000).
[51] A. Aoki, E. Kimura. *Chem. Rev*., **104**, 769 (2004).
[52] M. Gimeno, A. Laguna. In *Comprehensive Coordination Chemistry II*, J.A. McCleferty, T.J. Meyer (Eds), Vol. 6, Elsevier Pergamon, Oxford (2004).
[53] R. Österberg, B. Sjöberg. *J. Inorg. Nucl. Chem*., **37**, 815 (1975).
[54] R. Österberg, B. Sjöberg. *J. Biolog. Chem*., **243**, 3038 (1968).
[55] W. Beck. *Z. Naturforschung B*, **64**, 1221 (2009).
[56] S. Rajković, M. Ivković, C. Kállay, I. Sóvágó, M. Djuran. *Dalton Trans*., 8370 (2009).
[57] S. Barry, G. Rickard, M. Pushie, A. Rauk. *Can. J. Chem*., **87**, 942 (2009).
[58] F. Tureček, J. Jones, A. Holm, S. Panja, S. Nielsen, P. Hvelplund. *J. Mass Spectrom*., **44**, 707 (2009).
[59] A. Gergely, E. Farkas. *Dalton Trans*., 381 (1982).
[60] M. Martos, E. Carrasco. *Thermochim. Acta*, **54**, 361 (1982).
[61] D. Szalda, L. Marzilli, T. Kistenmacher. *Biochem. Biophys. Res. Comm*., **63**, 601 (1975).
[62] P. Reddy, P. Manjula, T. Chakraborty, R. Samanta. *Chem. Biodiversity*, **6**, 764 (2009).
[63] T. Shi, K. Siu, A. Hopkinson. *J. Phys. Chem. A*, **111**, 11562 (2007).
[64] K. Haas, W. Beck. *Z. Anorg. Allg. Chem*., **628**, 788 (2002).
[65] B. Schreiner, W. Beck. *Z. Anorg. Allg. Chem*., **636**, 499 (2010).
[66] W. Beck, W. Fehlhammer. *Z. Anorg. Allg. Chem*., **636**, 157 (2010).
[67] R. Gust, W. Beck, G. Jaouen, H. Schönenberger. *Coord. Chem. Rev*., **253**, 2742 (2009).
[68] R. Gust, W. Beck, G. Jaouen, H. Schönenberger. *Coord. Chem. Rev*., **253**, 2760 (2009).
[69] E. Schuhmann, W. Beck. *Z. Naturf*., **63**, 124 (2008).
[70] J. Schapp, K. Haas, K. Sünkel, W. Beck. *Eur. J. Inorg. Chem*., 3745 (2008).
[71] H. Dialer, K. Polborn, W. Ponikwar, K. Sünkel, W. Beck. *Chem. Eur. J*., **8**, 691 (2002).
[72] A. Stokes, Y. Xu, J. Daunais, H. Tamir, M. Gershon, P. Butkerait, B. Kayser, K. Vrana. *J. Neurochem*., **74**, 2067 (2001).
[73] K. Severin, W. Beck, G. Trojandt, K. Polborn, W. Steglich. *Angew. Chem. Int. Ed*., **34**, 1449 (2005).
[74] O. Hohage, W.S. Sheldrick. *J. Inorg. Biochem*., **100**, 1506 (2006).
[75] M. Hahn, M. Kleine, W.S. Sheldrick. *J. Biol. Inorg. Chem*., **6**, 556 (2001).
[76] M. Hahn, D. Wolters, W. Sheldrick, F. Hulsbergen, J. Reedijk. *J. Biol. Inorg. Chem*., **4**, 412 (1999).
[77] S. Robillard, A. Rob, P. Valentijn, N. Meeuwenoord, G. van der Marel, H. Jacques, W. van Boom, J. Reedijk. *Angew. Chem. Int. Ed*., **39**, 3096 (2006).
[78] R. Kannappan, D. Tooke, A. Spek, J. Reedijk. *J. Mol. Struct*., **751**, 55 (2005).
[79] K. Karidi, A. Garoufis, N. Hadjiliadis, J. Reedijk. *Dalton Trans*., 728 (2005).
[80] N. Jansen, B. van der Marel, G. van Boom, J. Reedijk. *New J. Chem*., **29**, 220 (2005).
[81] M. Robillard, M. Bacac, H. van den Elst, A. Flamigni, A. van der Marel, J. van Boom, J. Reedijk. *J. Comb. Chem*., **5**, 821 (2005).
[82] M. Robillard, N. Davies, G. van der Marel, J. van Boom, J. Reedijk, V. Murray. *J. Inorg. Biochem*., **96**, 331 (2005).
[83] K. Schmidt, M. Boudvillain, A. Schwartz, G. van der Marel, J. van Boom, J. Reedijk, B. Lippert. *Chem. Eur. J*., **8**, 5566 (2005).
[84] V. Aletras, N. Hadjiliadis, A. Karaliota, I. Rombeck, B. Lippert. *Inorg. Chim. Acta*, **227**, 17 (1994).
[85] M. Wienken, E. Zangrando, L. Randaccio, S. Menzer, B. Lippert. *Dalton Trans*., 3349 (1993).
[86] M. Wienken, B. Lippert, E. Zangrando, L. Randaccio. *Inorg. Chem*., **31**, 1983 (1992).
[87] B. Ivanova. *J. Coord. Chem*., **58**, 587 (2005).
[88] B. Ivanova, S. Todorov, A. Arnaudov. *J. Coord. Chem*., **59**, 1749 (2006).
[89] E. Hoffman. *Progress in Quantum Chemistry Research*, Nova Science Publishers, New York (2007).
[90] T. Kolev. *Biopolymers*, **83**, 39 (2006).
[91] B. Ivanova, T. Kolev, S. Zareva. *Biopolymers*, **82**, 587 (2006).
[92] B. Ivanova. *Spectrochim. Acta*, **64A**, 931 (2006).
[93] B. Ivanova, M. Arnaudov, S. Todorov, W. Sheldrick, H. Mayer-Figge. *Struct. Chem*., **17**, 49 (2006).
[94] B. Ivanova. *J. Mol. Struct*., **782**, 122 (2006).
[95] B. Koleva, T. Kolev, M. Spiteller. *Biopolymers*, **83**, 498 (2006).
[96] T. Kolev, B. Koleva, S. Zareva, M. Spiteller. *Inorg. Chim. Acta*, **359**, 4367 (2007).

[97] B. Koleva, T. Kolev, S. Todorov. *Chem. Papers*, **61**, 490 (2007).
[98] B. Koleva, T. Kolev, M. Spiteller. *Inorg. Chim. Acta*, **360**, 2224 (2007).
[99] B. Koleva, T. Kolev, S. Zareva, M. Spiteller. *J. Mol. Struct.*, **831**, 165 (2007).
[100] B. Koleva, S. Zareva, T. Kolev, M. Spiteller. *J. Coord. Chem.*, **61**, 3534 (2008).
[101] B. Koleva, T. Kolev, M. Lamshöft, M. Spiteller. *Transition Met. Chem.*, **33**, 911 (2008).
[102] B. Koleva, T. Kolev, S. Zareva, M. Spiteller. *J. Mol. Struct.*, **885**, 104 (2008).
[103] T. Kolev, B. Koleva, M. Spiteller. *J. Coord. Chem.*, **61**, 1897 (2008).
[104] S. Zareva, T. Kolev, A. Tchapkanov, M. Spiteller, B. Koleva. *Polish J. Chem.*, **83**, 421 (2009).
[105] T. Kolev, R. Seidel, H. Mayer-Figge, M. Spiteller, W. Sheldrick, B. Koleva. *Spectrochim. Acta*, **72A**, 502 (2009).
[106] A. Chapkanov, Y. Miteva, T. Kolev, M. Spiteller, B. Koleva. *Protein Pept. Lett.*, **17**, 228 (2010).
[107] B. Koleva, T. Kolev, R. Seidel, M. Spiteller, H. Mayer-Figge, W.S. Sheldrick. *J. Phys. Chem.*, **113A**, 3088 (2009).
[108] B. Koleva, T. Kolev, R. Seidel, H. Mayer-Figge, M. Spiteller, W. Sheldrick. *J. Phys. Chem.*, **112A**, 2899 (2008).
[109] B. Ivanova, M. Spiteller. *J. Phys. Chem.*, **114A**, 5099 (2010).
[110] B. Ivanova, M. Spiteller. *Cryst. Growth Des.*, **10**, 2470 (2010).
[111] T. Kolev, B. Koleva, R. Seidel, M. Spiteller, W. Sheldrick. *Cryst. Growth Des.*, **9**, 3348 (2009).
[112] K. Nakamoto. *Infrared and Raman Spectra of Inorganic and Coordination Compounds, Part I: Theory and Applications in Inorganic Chemistry*, Wiley, New York (1997).
[113] K. Nakamoto. *Infrared and Raman Spectra of Inorganic and Coordination Compounds, Part II: Applications in Coordination, Organometallic, and Bioinorganic Chemistry*, 5th Edn, Wiley, New York (1997).
[114] A. Biswas, E. Hughes, B. Sharma, J. Wilson. *Acta Crystallogr.*, **24B**, 40 (2968).
[115] R. Parthasarathy. *Acta Crystallogr.*, **25B**, 509 (1969).
[116] R. Meulemans, P. Piret, M. van Meerssche. *Acta Crystallogr.*, **27**, 1187 (1971).
[117] B. Strandberg, I. Lindqvist, R. Rosenstein. *Z. Kristallogr.*, **116**, 266 (1961).
[118] A. McLean, G. Chandler. *J. Chem. Phys.*, **72**, 5639 (1980).
[119] N. Nagao, T. Kobayashi, T. Takayama, Y. Koike, Y. Ono, T. Watanabe, T. Mikami, M. Suzuki, T. Matumoto, M. Watabe. *Inorg. Chem.*, **36**, 4195 (1997).
[120] M. Watabe, M. Kai, S. Asanuma, M. Yoshikane, A. Horiuchi, A. Ogasawara, T. Watanabe, T. Mikami, T. Matsumoto. *Inorg. Chem.*, **40**, 1496 (2001).
[121] R. Gillard, E. McKenzie, R. Mason, G.B. Robertson. *Nature (London)*, **209**, 1347 (1966).
[122] M. Cindric, T. Novak, S. Kraljevic, M. Kralj, B. Kamenar. *Inorg. Chim. Acta*, **359**, 1673 (2006).
[123] T. Yamase, M. Inoue, H. Naruke, K. Fukaya. *Chem. Lett.*, 563 (1999).
[124] C.B. Acland, H.C. Freeman. *J. Chem. Soc. D*, 1016 (1971).
[125] R. Kramer, M. Maurus, R. Bergs, K. Polborn, K. Sunkel, B. Wagner, W. Beck. *Chem. Ber.*, **126**, 1969 (1993).
[126] W. Sheldrick, S. Heeb. *J. Organomet. Chem.*, **377**, 357 (1989).
[127] M. Lipowska, L. Hansen, X. Xu, P. Marzilli, A. Taylor Jr, L. Marzilli. *Inorg. Chem.*, **41**, 3032 (2002).
[128] S. Rao, R. Parthasarathy. *Acta Crystallogr.*, **29B**, 2379 (1972).
[129] G. Freeman, R. Hearn, C. Bugg. *Acta Crystallogr.*, **28C**, 2906 (1972).
[130] E. Sudbeck, M. Etter, W. Gleason. *Chem. Mater.*, **6**, 1192 (1994).
[131] Z. Han, E. Wang, G. Luan, Y. Li, H. Zhang, Y. Duan, C. Hu, N. Hu. *J. Mater. Chem.*, **12**, 1169 (2002).
[132] L. Lenel. *Z. Kristallogr.*, **81**, 224 (1931).
[133] D. van der Helm, T. Willoughby. *Acta Crystallogr.*, **25**, 2317 (1969).
[134] V. Lalitha, E. Subramanian. *Cryst. Struct. Commun.*, **11**, 561 (1982).
[135] E. Handelsman-Benory, M. Botoshansky, M. Kaftory. *Acta Crystallogr.*, **51C**, 2362 (1995).
[136] M. Gordon, J. Binkley, J. Pople, W. Pietro, W. Hehre. *J. Am. Chem. Soc.*, **104**, 2797 (1982).
[137] K. Dobbs, W. Hehre. *J. Comp. Chem.*, **7**, 359 (1986).
[138] K. Dobbs, W. Hehre. *J. Comp. Chem.*, **8**, 861 (1987).
[139] K. Dobbs, W. Hehre. *J. Comp. Chem.*, **8**, 880 (1987).
[140] R. Ditchfield, W. Hehre, J. Pople. *J. Chem. Phys.*, **54**, 724 (1971).
[141] W. Hehre, R. Ditchfield, J. Pople. *J. Chem. Phys.*, **56**, 2257 (1972).
[142] P. Hariharan, J. Pople. *Mol. Phys.*, **27**, 209 (1974).
[143] M. Gordon. *Chem. Phys. Lett.*, **76**, 163 (1980).
[144] P. Hariharan, J. Pople. *Theor. Chim. Acta*, **28**, 213 (1981).
[145] J. Blaudeau, M. McGrath, L. Curtiss, L. Radom. *J. Chem. Phys.*, **107**, 5016 (1997).
[146] M. Francl, W. Pietro, W. Hehre, J. Binkley, D. DeFrees, J. Pople, M. Gordon. *J. Chem. Phys.*, **77**, 3654 (1982).
[147] R. Binning, L. Curtiss. *J. Comp. Chem.*, **11**, 1206 (1990).
[148] V. Rassolov, J. Pople, M. Ratner, T. Windus. *J. Chem. Phys.*, **109**, 1223 (1989).
[149] V. Rassolov, M. Ratner, J. Pople, P. Redfern, L. Curtiss. *J. Comp. Chem.*, **22**, 976 (1992).

[150] G. Petersson, A. Bennett, T. Tensfeldt, M. Laham, W. Shirley, J. Mantzaris. *J. Chem. Phys.*, **89**, 2193 (1988).
[151] A. McLean, G. Chandler. *J. Chem. Phys.*, **72**, 5639 (1982).
[152] R. Krishnan, J. Binkley, R. Seeger, J. Pople. *J. Chem. Phys.*, **72**, 650 (1980).
[153] A. Wachters. *J. Chem. Phys.*, **52**, 1033 (1970).
[154] P. Hay. *J. Chem. Phys.*, **66**, 4377 (1977).
[155] K. Raghavachari, G. Trucks. *J. Chem. Phys.*, **91**, 1062 (1989).
[156] L. Curtiss, M. McGrath, J. Blaudeau, N. Davis, R. Binning, L. Radom. *J. Chem. Phys.*, **103**, 6104 (1995).
[157] M. McGrath, L. Radom. *J. Chem. Phys.*, **94**, 511 (1991).
[158] C. Peng, P. Ayala, H. Schlegel, M. Frisch. *J. Comp. Chem.*, **17**, 49 (1996).
[159] R. Vargas, J. Garza, B. Hay, D. Dixon. *J. Phys. Chem.*, **106A**, 3213 (2002).
[160] G. Ramachandran, V. Sasisekharan. *Adv. Protein Chem.*, **23**, 283 (1968).
[161] S. Zimmerman, M. Pottle, G. Nemethy, H. Scherana. *Macromol.*, **10**, 1 (1977).
[162] O. Herzberg, J. Moult. *J. Proteins*, **11**, 223 (1991).
[163] D. Toroz, T. van Mourik. *Mol. Phys.*, **105**, 209 (2007).
[164] D. Toroz, T. van Mourik. *Mol. Phys.*, **104**, 559 (2006).
[165] G. Valle. *Eur. Cryst. Meeting*, **7**, 190 (1982).
[166] M. Bressan, R. Ettore, F. Marchiori, G. Valle. *Int. J. Pept. Protein Res.*, **19**, 402 (1972).
[167] T. Yamane, Y. Shiraishi, T. Ashida. *Acta Crystallogr.*, **41C**, 946 (1985).
[168] R. Stenkamp, L. Jensen. *Acta Crystallogr.*, **31B**, 857 (1972).
[169] R. Bergs, K. Sunkel, C. Robl, W. Beck. *J. Organomet. Chem.*, **533**, 247 (1997).
[170] C. Giordano, G. Lucente, A. Mollica, M. Nalli, G.P. Zecchini, M.P. Paradisi, E. Gavuzzo, F. Mazza, S. Spisani. *J. Pept. Sci.*, **10**, 510 (2004).
[171] A. Jimenez, C. Cativiela, M. Marraud. *Tetrahedron Lett.*, **41**, 5353 (2000).
[172] D. Shi, T.W. Hambley, H.C. Freeman. *Inorg. Biochem.*, **73**, 173 (1999).
[173] L. Pasternak. *Acta Crystallogr.*, **5**, 152 (1952).
[174] B. Rajkumar, V. Ramakrishnan. *Spectrochim. Acta*, **58A**, 1923 (2002).
[175] M. Gerhards. *Phys. Chem. Chem. Phys.*, **4**, 1760 (2002).
[176] E. Tsuboi, Z. Ezaki, M. Aida, A. Yimit, K. Ushiza, U. Ueda. *Biospectroscopy*, **4**, 61 (1998).
[177] Z. Arp, D. Autrey, J. Laane, S. Overman, J. Thomas. *Biochemistry*, **40**, 2522 (2001).
[178] I. Wawer, S. Witkowski. *Curr. Org. Chem.*, **5**, 987 (2001).
[179] P. Hajduk, D. Augeri, J. Mack, R. Mendoza, J. Yang, S. Betz, S. Fesik. *J. Am. Chem. Soc.*, **122**, 7898 (2000).
[180] H. Schwalbe, J. Wermuth, C. Richter, S. Szalma, A. Eschenmoser, G. Quinkert. *Helv. Chim. Acta*, **83**, 1079 (2000).
[181] C. Beguin, S. Hamman. *Org. Mag. Res.*, **16**, 129 (1981).
[182] J. MacDonald. *Can. J. Mag. Res.*, **34**, 207 (1979).
[183] M. Kainosho, K. Ajisaka. *J. Am. Chem. Soc.*, **97**, 5630 (1975).
[184] J. Feeney, P. Hansen, C. Roberts. *Chem. Commun.*, 465 (1974).
[185] A. Piccolo, M. Spiteller. *Anal. Bioanal. Chem.*, **377**, 1047 (2003).
[186] C. McIntyre, B. Batts, D. Jardine. *J. Mass. Spectrom.*, **32**, 328 (1997).
[187] U. Klaus, T. Pfeifer, M. Spiteller. *Environ. Sci. Technol.*, **34**, 3514 (2000).
[188] T. Pfeifer, K. Uwe, R. Hoffmann, M. Spiteller. *J. Chrom.*, **926**, 151 (2001).
[189] E. Cole. *J. Mass Spectrom.*, **35**, 763 (2000).
[190] L. Brown, J.A. Rice. *Anal. Chem.*, **72**, 384 (2000).
[191] D. Morgan, M. Bursey. *J. Mass Spectrom.*, **30**, 290 (1995).
[192] Y. Wang, Y. Ke, F. Siu, K. Guevremont. *J. Mass Spectrom.*, **31**, 34 (1996).
[193] S. Carr, C. Cassady. *J. Mass Spectrom.*, **32**, 959 (1997).
[194] Z. Li, T. Yalcin, C. Cassady. *J. Mass Spectrom.*, **41**, 939 (2006).
[195] B. Biemann, S. Martin. *Mass Spectrom. Rev.*, **6**, 1 (1987).
[196] Y. Tomuka, T. Ashida, M. Kakudo. *Acta Crystallogr.*, **25B**, 1367 (1969).
[197] T. Tranter. *Nature (London)*, **177**, 37 (1956).
[198] P. Naganathan, K. Venkatesan. *Acta Crystallogr.*, **28B**, 552 (1972).
[199] T. Tranter. *Nature (London)*, **173**, 221 (1954).
[200] Y. Tomuka, T. Ashida, M. Kakudo. *Acta Crystallogr.*, **25B**, 1367 (1979).
[201] Q. Hu, R. Noll, H. Li, A. Makarov, M. Hardman, R. Graham Cooks. *J. Mass Spectrom.*, **40**, 430 (2005).
[202] A. Moen, M. Froseth, C. Görbitz, B. Dalhus. *Acta Crystallogr.*, **60C**, o564 (2004).
[203] J. Slowikowska, J. Lipkowski. *Acta Crystallogr.*, **57C**, 187 (2001).
[204] V. Yadava, V. Padmanabhan. *Acta Crystallogr.*, **29C**, 854 (1973).
[205] E. Subramanian, R. Murali, J. Trotter. *Curr. Sci.*, **52**, 995 (1983).
[206] M. Cotrait, Y. Barrans, F. Leroy. *Acta Crystallogr.*, **38B**, 1626 (1982).
[207] G. Grant, A. Hunt, P. Milne, H. Roos, J. Joubert. *J. Chem. Cryst.*, **29**, 435 (1999).

[208] T. Steiner, A. Schreurs, J. Kanters, J. Kroon. *Acta Crystallogr*., **54D**, 25 (1998).
[209] T. Emge, A. Agrawal, J. Dalessio, G. Dukovic, J. Inghrim, K. Janjua, M. Macaluso, L. Robertson, T. Stiglic, Y. Volovik, M. Georgiadis. *Acta Crystallogr*., **56C**, e469 (2000).
[210] M. Cotrait, P. Bideau. *Acta Crystallogr*., **30B**, 1024 (1974).
[211] A. Mostad, H. Nissen, C. Romming. *Acta Chem. Scand*., **26**, 3819 (1972).
[212] M. Frey, T. Koetzle, M. Lehmann, W. Hamilton. *J. Chem. Phys*., **58**, 2547 (1973).
[213] M. Hursthouse, S.A.A. Jayaweera, H. Milburn, A. Quick. *Dalton Trans*., 2569 (1975).
[214] P. Angelo, E. Bottari, M. Festa, H. Nolting, N. Pavel. *J. Phys. Chem*., **102B**, 3114 (1998).
[215] K. Ozitsumi, Y. Yamaguchi, T. Ohtaki, K. Tohji, Y. Udagawa. *Bull. Chem. Soc. Japan*, **58**, 2786 (1985).
[216] T. Bruin, A. Marcelis, H. Zuilhof, E. Sudhölter. *Phys. Chem. Chem. Phys*., **1**, 4157 (1999).
[217] A. Spisni, G. Sartor, L. Franzoni, A. Orsolini, P. Cavatorta. *Bull. Mag. Res*., **14**, 165 (1990).
[218] M. Tabak, G. Sartor, P. Cavatorta. *J. Luminesc*., **43**, 355 (1989).
[219] M. Tabak, G. Sartor, P. Neyroz, P. Cavatorta. *J. Luminesc*., **46**, 291 (1990).
[220] J. Jeon, S. Yang, J. Choi, M. Cho. *Acc. Chem. Res*., **42**, 1280 (2009).
[221] L. Kirschenbaum, J. Rush. *J. Am. Chem. Soc*., **106**, 1003 (1984).
[222] O. Yamauchi. *Pure Appl. Chem*., **67**, 297 (1995).
[223] V. Rajasekharapinl, M. Mutter. *Acc. Chem. Res*., **14**, 122 (1981).
[224] Y. Kawashima, T. Usami, N. Ohashi, R. Suenram, J. Hougen, E. Hirota. *Acc. Chem. Res*., **39**, 216 (2006).
[225] A. Vallee, V. Humblot, C. Pradier. *Acc. Chem. Res*., **43**, 1297 (2010).
[226] T. Lovell, F. Himo, W. Han, L. Noodleman. *Coord. Chem. Rev*., **238**, 211/232 (2003).
[227] X. Assfeld, N. Ferré, J. Rivail. *Theor. Chem. Acc*., **111**, 328 (2004).
[228] L. Estévez, N. Otero, R. Mosquera. *Theor. Chem. Acc*. DOI: 10.1007/s00214-010-0829-0.
[229] G. Brancolini, A. Venturini, F. Zerbetto. *Theor. Chem. Acc*., **118**, 25 (2007).
[230] M. Brown, B. Gherman. *Theor. Chem. Acc*. DOI: 10.1007/s00214-010-0827-2.
[231] P. Politzer. In *Chemical Applications of Atomic and Molecular Potentials*, P. Politzer, D. Truhlar (Eds), pp. 7–28, Plenum Press, New York (1981).
[232] Y. Zhao, D. Truhlar. *Acc. Chem. Res*., **41**, 157 (2008).
[233] F. de Proft, P. Geerlings. *Chem. Rev*., **101**, 1451 (2001).